

Supervised Dimensionality Reduction for Big Data

Joshua T. Vogelstein^{1*†}, Eric W. Bridgeford^{1*}, Minh Tang¹, Da Zheng¹, Christopher Douville¹, Randal Burns¹, Mauro Maggioni¹

¹ Johns Hopkins University, *Co-First, †Corresponding Author

To solve key biomedical problems, experimentalists now routinely measure millions or billions of features (dimensions) per sample, with the hope that data science techniques will be able to build accurate data-driven inferences. Because sample sizes are typically orders of magnitude smaller than the dimensionality of these data, valid inferences require finding a low-dimensional representation that preserves the discriminating information (e.g., whether the individual suffers from a particular disease). There is a lack of interpretable supervised dimensionality reduction methods that scale to millions of dimensions with strong statistical theoretical guarantees. We introduce an approach, XOX, to extending principal components analysis by incorporating class-conditional moment estimates into the low-dimensional projection. The simplest version, “Linear Optimal Low-rank” projection (LOL), incorporates the class-conditional means. We prove, and substantiate with both synthetic and real data benchmarks, that LOL and its generalizations in the XOX framework lead to improved data representations for subsequent classification, while maintaining computational efficiency and scalability. Using multiple brain imaging datasets consisting of >150 million features, and several genomics datasets with >500,000 features, LOL outperforms other scalable linear dimensionality reduction techniques in terms of accuracy, while only requiring a few minutes on a standard desktop computer.

Supervised learning—the art and science of estimating statistical relationships using labeled training data—has enabled a wide variety of basic and applied findings, ranging from discovering biomarkers in omics data [72] to recognizing objects from images [50]. A special case of supervised learning is classification, where a classifier predicts the “class” of a novel observation (for example, by predicting sex from an MRI scan). One of the most foundational and important approaches to classification is Fisher’s Linear Discriminant Analysis (LDA) [35]. LDA has a number of highly desirable properties for a classifier. First, it is based on simple geometric reasoning: when the data are Gaussian, all the information is in the means and variances, so the optimal classifier uses both the means and the variances. Second, LDA can be applied to multiclass problems. Third, theorems guarantee that when the sample size n is large and the dimensionality p is relatively small, LDA converges to the optimal classifier under the Gaussian assumption. Finally, algorithms for implementing it are highly efficient.

Modern scientific datasets, however, present challenges for classification that were not addressed in Fisher’s era. Specifically, the dimensionality of datasets is quickly ballooning. Current raw data can consist of hundreds of millions of features or dimensions; for example, an entire genome or connectome. Yet, the sample sizes have not experienced a concomitant increase. This “large p , small n ” problem is a non-starter for many classical statistical approaches because they were designed with a “small p , large n ” situation in mind. Running LDA when $p \geq n$ is like trying to fit a line to a point: there are infinitely many equally good fits (all lines that pass through the point), and no way to know which of them is “best”. Therefore, without further constraints these algorithms will overfit, meaning they will choose a classifier based on noise in the data, rather than discarding the noise in favor of the desired signal. We also desire methods that can adapt to the complexity of the data, are robust to outliers, and are computationally efficient. Several complementary strategies have been pursued to address these $p \geq n$ problems.

First, and perhaps the most widely used method, is Principal Components Analysis (PCA) [48]. Accord-

ing to PubMed, PCA has been referenced over 40,000 times, and nearly 4,000 times in 2018 alone. This is in contrast to other methods that receive much more attention in the media, such as deep learning, random forests, and sparse learning, which received $\sim 2,000$, $\sim 1,200$ and ~ 500 hits, respectively. This suggests that PCA remains the most popular workhorse for high-dimensional problems. PCA “pre-processes” the data by reducing its dimensionality to those dimensions whose variance is largest in the dataset. While highly successful, PCA is a wholly *unsupervised* dimensionality reduction technique, meaning that PCA does not use the class labels while learning the low-dimensional representation, resulting in sub-optimal performance for subsequent classification. Nonlinear manifold learning techniques generalize PCA [54], but also typically do not incorporate class label information; moreover, they scale poorly. Deep learning provides the most recent version of nonlinear manifold learning, for example, using (supervised) autoencoders, but these methods remain poorly understood, have many parameters to tune, and typically do not provide interpretable results [38]. Further, deep learning tends to suffer in the wide data problem, where the number of samples is far less than the dimensionality.

The second set of strategies regularize or penalize a supervised method, such as regularized LDA [73] or canonical correlation analysis (CCA) [64]. Such approaches can drastically overfit in the $p > n$ setting, tend to lack theoretical support in these contexts, and have multiple “knobs” to tune that are computationally taxing. Partial least squares (PLS) is another popular method in this set that often achieves impressive empirical performance, though it lacks strong theoretical guarantees and a scalable implementation [16, 67]. Sparse methods are the third common strategy to mitigate this “curse of dimensionality” [34, 45, 68]. Unfortunately, exact solutions are computationally intractable, and approximate solutions have theoretical guarantees only under very restrictive assumptions, and are quite fragile to those assumptions [66]. Thus, there is a gap: no existing approach can classify multi-class wide data with millions of features while obtaining strong theoretical guarantees, favorable and interpretable empirical performance, and a flexible, robust, and scalable implementation.

To address these issues, we developed a technique for incorporating class-conditional moment estimates, XOX , the simplest example of which is LOL . *The key intuition behind LOL is that we can jointly use the means and variances from each class (like LDA and CCA), but without requiring more dimensions than samples (like PCA), or restrictive sparsity assumptions.* Using random matrix theory, we are able to prove that when the data are sampled from a Gaussian, LOL finds a better low-dimensional representation than PCA , LDA , CCA , and other linear methods. Under relatively relaxed assumptions, this is true regardless of the dimensionality of the features, the number of samples, or the number of dimensions in which we project. We then demonstrate the superiority of techniques derived using the XOX approach—including (i) LOL , (ii) a variant of XOX which allows greater flexibility of the class-conditional covariances called QOQ , and (iii) a robust variant of LOL called $RLOL$ —over other methods numerically on a variety of simulated settings including several not following the theoretical assumptions. Finally, we show that on several 500 gigabyte neuroimaging datasets, and several multi-gigabyte genomics datasets, LOL achieves superior accuracy at lower dimensions while requiring only a few minutes of time on a single workstation.

Supervised Manifold Learning

A general strategy for supervised manifold learning is schematized in Figure 1, and outlined here. Step **(A)**: Obtain or select n training samples of high-dimensional data. For concreteness, we use one of the most popular benchmark datasets, the MNIST dataset [53]. This dataset consists of images of hand-written digits 0 through 9. Each image is represented by a 28×28 matrix, which means that the observed dimensionality of the data is $p = 28^2 = 784$. Because we are motivated by the $n \ll p$

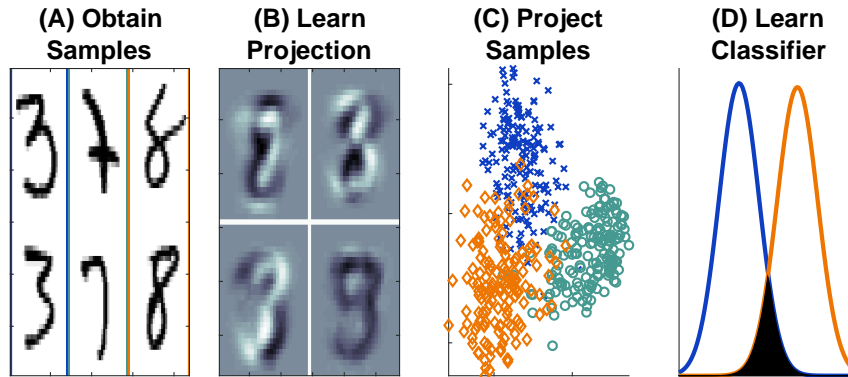


Figure 1: Schematic illustrating Linear Optimal Low-rank (LOL) as a supervised manifold learning technique. **(A)** 300 training samples of the numbers 3, 7, and 8 from the MNIST dataset (100 samples per digit); each sample is a $28 \times 28 = 784$ dimensional image (boundary colors are for visualization purposes). **(B)** The first four projection matrices learned by LOL. Each is a linear combination of the sample images. **(C)** Projecting 500 new (test) samples into the top two learned dimensions; digits color coded as in (A). LOL-projected data from three distinct clusters. **(D)** Using the low-dimensional data to learn a classifier. The estimated distributions for 3 and 8 of the test samples (after projecting data into two dimensions and using LDA to classify) demonstrate that 3 and 8 are easily separable by linear methods after LOL projections (the color of the line indicates the digit). The filled area is the estimated error rate; the goal of any classification algorithm is to minimize that area. LOL is performing well on this high-dimensional real data example.

scenario, we subsample the data to select $n = 300$ examples of the numbers 3, 7, and 8 (100 of each). **Step (B):** Learn a “projection” that maps the high-dimensional data to a low-dimensional representation. One can do so in a way that ignores which images correspond to which digit (the “class labels”), as PCA and most manifold learning techniques do, or try to use the labels, as LDA and sparse methods do. LOL is a supervised linear manifold learning technique that uses the class labels to learn projections that are linear combinations of the original data samples. **Step (C):** Use the learned projections to map high-dimensional data into the learned lower-dimensional space. This step requires having learned a projection that can be applied to new (test) data samples for which we do not know the true class labels. Nonlinear manifold learning methods typically cannot be applied in this way (though see [12]). LOL, however, can project new samples in such a way as to separate the data into classes. **Step (D):** Using the low-dimensional representation of the data, learn a classifier. A good classifier correctly identifies as many points as possible with the correct label. For these data, when LDA is used on the low-dimensional data learned by LOL, the data points are mostly linearly separable, yielding a highly accurate classifier.

The Geometric Intuition of LOL

To build intuition for situations when LOL performs well, and when it does not, we consider the simplest high-dimensional classification setting. We observe n samples (\mathbf{x}_i, y_i) , where \mathbf{x}_i are p dimensional feature vectors, and y_i is the binary class label, that is, y_i is either 0 or 1. We assume that both classes are distributed according to a multivariate Gaussian distribution, the two classes have the same identity covariance matrix (all features are uncorrelated with unity variance), and data from either class is equally likely, so that the only difference between the classes is their means. In this scenario, the optimal low-dimensional projection is analytically available: it is the dot product of the difference of means and the inverse covariance matrix, commonly referred to as Fisher’s Linear Discriminant Analysis (LDA)

[13] (see Appendix A for derivation). When the distribution of the data is unavailable, as in all real data problems, machine learning methods can be used to estimate the parameters. Unfortunately, when $n < p$, the estimated covariance matrix will not be invertible (because the solution to the underlying mathematical problem is under specified), so some other approach is required. As mentioned above, PCA is commonly used to learn a low-dimensional representation. PCA uses the pooled sample mean and the pooled sample covariance matrix. The PCA projection is composed of the top d eigenvectors of the pooled sample covariance matrix, after subtracting the pooled mean (thereby completely ignoring the class labels).

In contrast, LOL uses the class-conditional means and class-centered covariance. This approach is motivated by Fisher’s LDA, which uses the same two terms, and should therefore improve performance over PCA. More specifically, for a two-class problem, LOL is constructed as follows:

1. Compute the sample mean of each class.
2. Estimate the difference between means.
3. Compute the class-centered covariance matrix, that is, compute the covariance matrix after subtracting the class mean from each point.
4. Compute the eigenvectors of this class-conditionally centered covariance.
5. Concatenate the difference of the means with the top $d - 1$ eigenvectors of class-centered covariance.

Note that the sample class-centered covariance matrix estimates the population covariance, colored—whereas the sample pooled covariance matrix is distorted by the difference of the class means. Further, as discussed in Appendix D, the class-centered covariance matrix is equivalent to “Reduced Rank LDA” [42] (rrLDA hereafter, which is simply LDA but truncating the covariance matrix). For the theoretical background on LDA and rrLDA, a formal definition of LOL, and detailed description of the simulation settings that follow, see Appendices A, B, and C, respectively. Figure 2 shows three different examples of 100 data points sampled from a 1,000 dimensional Gaussian to geometrically illustrate the intuition that motivated LOL. In each case, all dimensions are uncorrelated with one another, and all classes are equally likely with the same covariance; the only difference between the classes are their means.

Figure 2A shows “stacked cigars”, in which the difference between the means and the direction of maximum variance are large and aligned with one another. This is an idealized setting for PCA, because PCA finds the direction of maximal variance, which happens to correspond to the direction of maximal separation of the classes. rrLDA performs well here too, for the same reason that PCA does. Because all dimensions are uncorrelated, and one dimension contains most of the information discriminating between the two classes, this is also an ideal scenario for sparse methods. Indeed, ROAD, a sparse classifier designed for precisely this scenario, does an excellent job finding the most useful dimensions [34]. LOL, using both the difference of means and the directions of maximal variance, also does well. To calibrate all of these methods, we also show the performance of the optimal classifier.

Figure 2B shows an example that is worse for PCA. In particular, the variance is getting larger for subsequent dimensions, while the magnitude of the difference between the means is decreasing with dimension. Because PCA operates on the pooled sample covariance matrix, the dimensions with the maximum difference are included in the estimate, and therefore, PCA finds some of them, while also finding some of the dimensions of maximum variance. The result is that PCA performs fairly well in this setting. rrLDA, however, by virtue of subtracting out the difference of the means, is now completely at chance performance. ROAD is not hampered by this problem; it is also able to find the directions of maximal discrimination, rather than those of maximal variance. Again, LOL, by using both the means and the covariance, does extremely well.

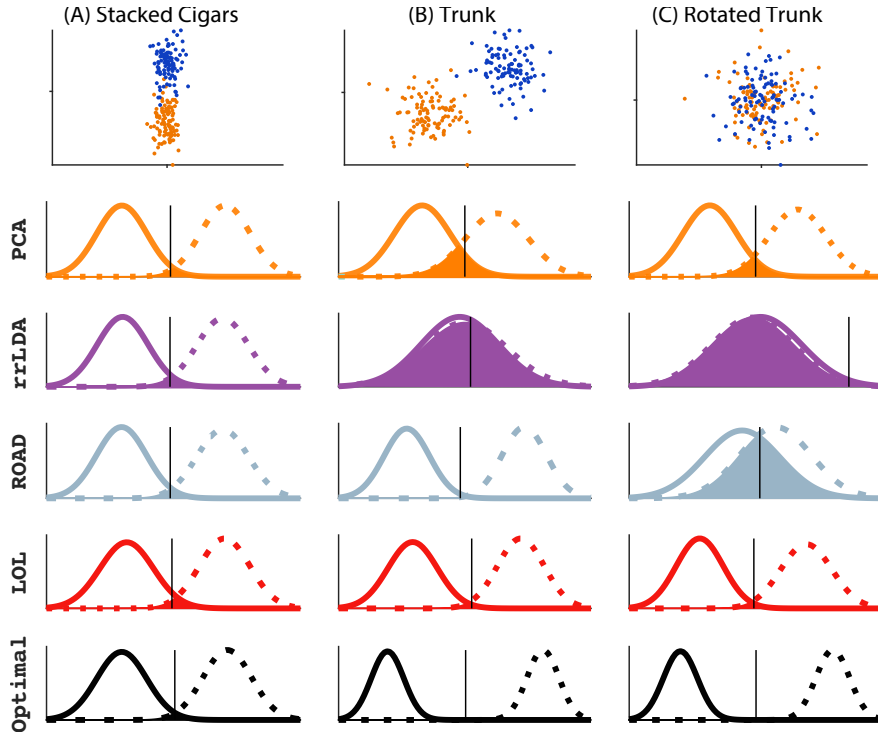


Figure 2: LOL achieves near-optimal performance for three different multivariate Gaussian distributions, each with 100 samples in 1000 dimensions. For each approach, we project into the top 3 dimensions, and then use LDA to classify 10,000 new samples. The six rows show (from top to bottom): *Row 1:* A scatter plot of the first two dimensions of the sampled points, with class 0 and 1 as orange and blue dots, respectively. The next rows each show the estimated posterior for class 0 and class 1, in solid and dashed lines, respectively. The overlap of the distributions—which quantifies the magnitude of the error—is filled. The black vertical line shows the estimated threshold for each method. The techniques include: PCA; reduced rank LDA (rrLDA), a method that projects onto the top d eigenvectors of sample class-conditional covariance; ROAD, a sparse method designed specifically for this model; LOL, our proposed method; and the Bayes optimal classifier. **(A) Stacked Cigars** The mean difference vector is aligned with the direction of maximal variance, and is mostly concentrated in a single dimension, making it ideal for PCA, rrLDA, and sparse methods. In this setting, the results are similar for all methods, and essentially optimal. **(B) Trunk** The mean difference vector is orthogonal to the direction of maximal variance; PCA performs worse and rrLDA is at chance, but sparse methods and LOL can still recover the correct dimensions, achieving nearly optimal performance. **(C) Rotated Trunk** Same as (B), but the data are rotated; in this case, only LOL performs well. Note that LOL is closest to Bayes optimal in all three settings.

Figure 2C is exactly the same as Figure 2B, except the data have been randomly rotated in all 1000 dimensions. This means that none of the original features have much information, but rather, linear combinations of them do. This is evidenced by observing the scatter plot, which shows that the first two dimensions fail to disambiguate the two classes. PCA performs even worse in this scenario than in the previous one. rrLDA is rotationally invariant (see Appendix B.IV for details), so still performs at chance levels. Because there is no small number of features that separate the data well, ROAD fails. LOL performs as well here as it does in the other examples.

When is LOL Better than PCA and Other Supervised Linear Methods?

We desire theoretical confirmation of the above numerical results. To do so, we investigate when LOL is “better” than other linear dimensionality reduction techniques. In the context of supervised dimension-

ality reduction or manifold learning, the goal is to obtain low dimensional representation that maximally separates the two classes, making subsequent classification easier. Chernoff information quantifies the dissimilarity between two distributions. Therefore, we can compute the Chernoff information between distribution of the two classes after embedding to evaluate the quality of a given embedding strategy. As it turns out, Chernoff information is the exponential convergence rate for the Bayes error [23], and therefore, the tightest possible theoretical bound. The use of Chernoff information to theoretically evaluate the performance of an embedding strategy is novel, to our knowledge, and leads to the following main result:

Main Theoretical Result *LOL is always better than or equal to rrLDA under the Gaussian model when $p \geq n$, and better than or equal to PCA (and many other linear projection methods) with additional (relatively weak) conditions. This is true for all possible observed dimensionalities of the data, and the number of dimensions into which we project, for sufficiently large sample sizes. Moreover, under relatively weak assumptions, these conditions almost certainly hold as the number of dimensions increases.*

Formal statements of the theorems and proofs required to substantiate the above result are provided in Appendix D. The condition for LOL to be better than PCA is essentially that the d^{th} eigenvector of the pooled sample covariance matrix has less information about classification than the difference of the means vector. The implication of the above theorem is that it is better to incorporate the mean difference vector into the projection matrix, rather than ignoring it, under basically the same assumptions that motivate PCA. The degree of improvement is a function of the dimensionality of the feature set p , the number of samples n , the projection dimension d , and the parameters, but the existence of an improvement—or at least no worse performance—is independent of those factors.

Flexibility and Accuracy of XOX Framework

We empirically investigate the flexibility and accuracy of XOX using simulations that extend beyond the theoretical claims. For three different scenarios, we sample 100 training samples each with 100 features; therefore, Fisher’s LDA cannot solve the problem (because there are infinitely many ways to overfit). We consider a number of different methods, including PCA, rrLDA, PLS, ROAD, Random Projections (RP), and CCA to project the data onto a low dimensional space. After projecting the data, we train either LDA (for the first two scenarios) or Quadratic Discriminant Analysis (QDA, for the third scenario), which generalizes LDA by allowing each class to have its own covariance matrix [43]. For each scenario, we evaluate the misclassification rate on held-out data.

Figure 3 shows a two-dimensional scatterplot (left) and misclassification rate versus dimensionality (right) for each simulation. The top $C - 1$ embedding dimensions for LOL correspond to the performance after projection onto the class-conditional means, and rrLDA corresponds to the performance of projection onto the class-conditional covariance matrix. Figure 3A shows a three class generalization of the Trunk example from Figure 2B. LOL can trivially be extended to more than two classes (see Section B for details), unlike ROAD which only operates in a two-class setting. Figure 3B shows a two-class example with many outliers, as is typical in modern biomedical datasets. A variant of LOL, “Robust LOL” (RLOL), replaces the standard estimators of the mean and covariance with robust variants (the class-conditional medians and robust covariance [27] respectively), thereby dramatically improving performance over LOL (and other techniques) in noisy settings. Hereafter, LOL will refer to the version of LOL with a robust estimate of the first moment, and a truncated estimate of the second moment, as a robust first moment tends to make little difference when a robust estimate was not necessary, and improved performance when a robust estimate was warranted. We do not use a robust estimate of

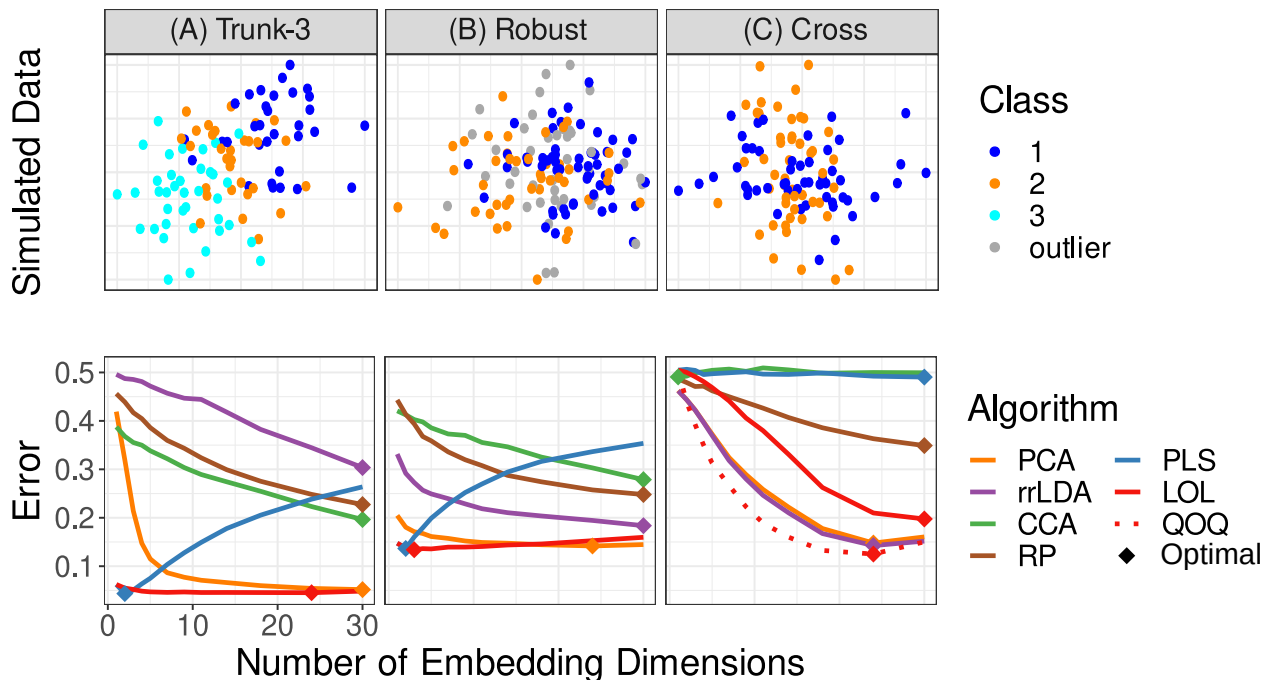


Figure 3: Three simulations demonstrating the flexibility and accuracy of xox in settings beyond current theoretical claims. For all cases, training sample size and dimensionality were both 100. The top row depicts the values of the sampled points for two of the 100 dimensions to illustrate the classification task. The bottom row misclassification rate as a function of the number of projected dimensions, for several different embedding approaches. Classification is performed on the embedded data using the LDA classifier for (A) and (B), and using QDA for (C). The simulation settings are: **(A) Trunk-3** A variation of Figure 2(B) in which 3 classes are present. **(B) Robust** Outliers are prominent in the sample while estimating the projection matrix. LOL is robust to the outliers due to the robust estimate of the first moment. **(C) Cross** The two classes have the same mean but orthogonal covariances. Points are classified using the QDA classifier after projection. QOQ, a variant of LOL where each class’ covariance is incorporated into the projection matrix, outperforms other methods, as expected. In essentially all cases and dimensions, LOL, or the appropriate generalization thereof, outperforms other approaches.

the second moment, as typical robust estimates of the second moment available in standard numerical packages require $d < n$. which is unsuitable for wide data. Figure 3C shows an example that does not have an effective linear discriminant boundary because the two classes have orthogonal covariances. Another variant of LOL, Quadratic Optimal QDA (QOQ), computes the eigenvectors separately for each class, concatenates them (sorting them according to their singular values), and then classifies with QDA instead of LOL. For all three scenarios, either LOL—or its extended variants RLOL and QOQ—achieves a misclassification rate comparable to or lower than other methods, for all dimensions. These three results demonstrate how straightforward generalizations of LOL under the xox framework which incorporate alternate or robust moment estimates can dramatically improve performance over other projection methods. This is in marked contrast to other approaches, for which such flexibility is either not available, or otherwise problematic.

xox is Computationally Efficient and Scalable

When the dimensionality is large (e.g., millions or billions), the main bottleneck is sometimes merely the ability to run anything on the data, rather than its predictive accuracy. We evaluate the computational efficiency and scalability of LOL in the simplest setting: two classes of spherically symmetric Gaus-

sians (see Appendix C for details) with dimensionality varying from 2 million to 128 million, and 1000 samples per class. Because LOL admits a closed form solution, it can leverage highly optimized linear algebra routines rather than the costly iterative programming techniques currently required for sparse or dictionary learning type problems [58]. To demonstrate these computational capabilities, we built FlashLOL, an efficient scalable LOL implementation with R bindings, to complement the R package used for the above figures.

Four properties of LOL enable its scalable implementation. First, LOL is linear in both sample size and dimensionality (Figure 4A, solid red line). Second, LOL is easily parallelizable using recent developments in “semi-external memory” [75–77] (Figure 4A, dashed red line demonstrates that LOL is also linear in the number of cores). Also note that LOL does not incur any meaningful additional computational cost over PCA (orange dashed line). Third, LOL can use randomized approximate algorithms for eigendecompositions to further accelerate its performance [20, 44] (Figure 4A, orange lines). FlashLFL, short for Flash Low-rank Fast Linear embedding, achieves an order of magnitude improvement in speed when using very sparse random projections instead of the eigenvectors. Fourth, hyper-parameter selection for LOL is nested, meaning that once estimating the d -dimensional projection, every lower dimensional projection is automatically available. This is in contrast to tuning the weight of a penalty term, which leads to a new optimization problem for each different parameter values. Thus, the computational complexity of LOL is $\mathcal{O}(npd/Tc)$, where n is sample size, p is the dimension of the data, d is the dimension of the projection, T is the number of threads, and c is the sparsity of the projection.

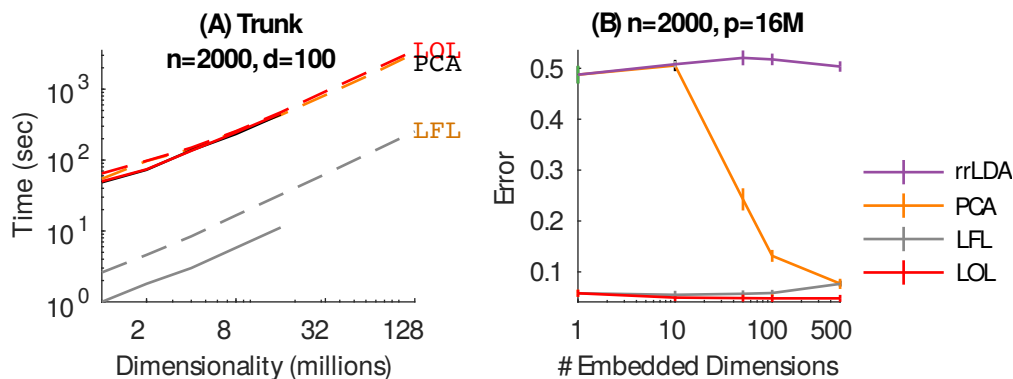


Figure 4: Computational efficiency and scalability of LOL using $n = 2000$ samples from spherically symmetric Gaussian data (see Appendix C for details). **(A)** LOL exhibits optimal (linear) scale up, requiring only 46 minutes to find the projection on a 500 gigabyte dataset, and only 3 minutes using LFL (dashed lines show semi-external memory performance). **(B)** Error for LFL is the same as LOL in this setting, and both are significantly better than PCA and rrLDA for all choices of projection dimension, regardless of whether a randomized approach is used to compute the projection dimensions.

Finally, note that this simulation setting is ideal for PCA and rrLDA, because the first principal component includes the mean difference vector. Nonetheless, both LOL and LFL achieve near optimal accuracy, whereas rrLDA is at chance, and PCA requires 500 dimensions to even approach the same accuracy that LOL achieves with only one dimension. While PCA would also benefit efficiency wise from a randomized approach, we emphasize that LFL maintains the high performance of LOL in comparison to PCA despite the randomization technique, with the benefit of greater computational efficiency compared to LOL.

Real Data Benchmarks and Applications

Real data often break the theoretical assumptions in more varied ways than the above simulations, and can provide a complementary perspective on the performance properties of different algorithms. We describe two sets of problems, one from brain imaging, and the other from genomics. In both cases we consider a classification problem. To classify participants, researchers typically employ substantive pre-processing pipelines [18] to reduce the dimensionality of the data. Unfortunately, as debates persist about the validity of pre-processing approaches, there is no defacto “standard” for the optimal strategies to pre-process the data. Traditional approaches typically include a deep processing chain, with many steps of parametric modeling and downsampling [39, 40, 49]. We therefore investigate the possibility of directly classifying on the nearly raw, high-dimensional data.

The Consortium for Reliability and Reproducibility (CoRR) [78] has generated anatomical and diffusion magnetic resonance imaging scans from $n > 800$ participants from 5 processing sites, each featuring participant-specific annotations for the sex of each individual. At the native resolution, each brain volume is over 150 million dimensions, and each dataset consists of between 42 (60 GB of data) and > 400 samples (600 GB of data).

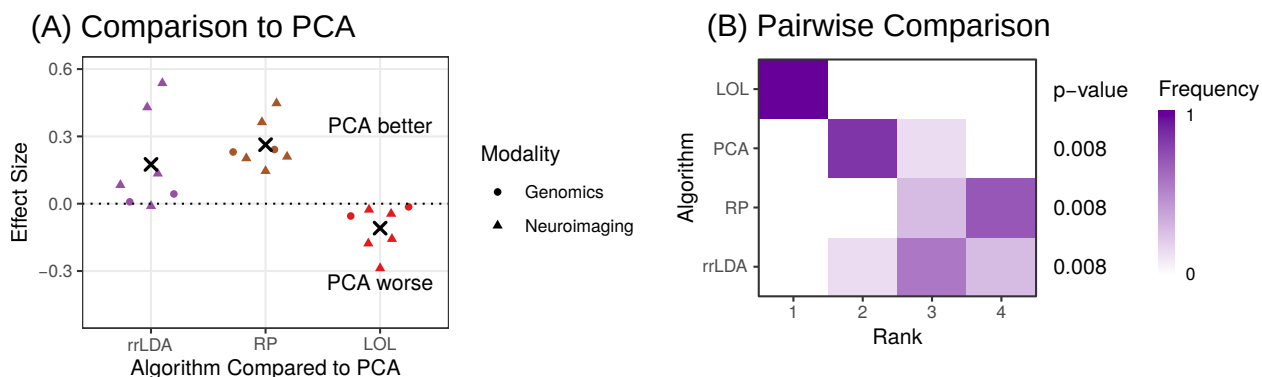


Figure 5: Comparing various dimensionality reduction algorithms on two real datasets: neuroimaging and genomics. **(A)** Beeswarm plots show the classification performance of each technique with respect to PCA at the optimal number of embedding dimensions, the number of embedding dimensions with the lowest misclassification rate. Performance is measured by the effect size, defined as $\kappa(LDA \circ PCA) - \kappa(LDA \circ embed)$, where κ is Cohen’s Kappa, and $embed$ is one of the embedding techniques compared to PCA . Each point indicates the performance of PCA relative the other technique on a single dataset, and the sample size-weighted average effect is indicated by the black “x.” LOL always outperforms PCA and all other techniques. **(B)** Frequency histograms of the relative ranks of each of the embedding techniques on each dataset after classification, where a 1 indicates the best relative classification performance and a 4 indicates the worst relative classification performance, after embedding with the technique indicated. Projecting first with LOL provides a significant improvement over competing strategies (Wilcoxon signed-rank test, $n = 7$, p -value=.008) on all benchmark problems.

We then also consider a large genomics dataset [31] consisting of 340 individuals: 144 patients with non-metastatic cancer and 196 healthy controls, of which 198 are male and 142 are female. Samples are aligned to $>750,000$ amplicons distributed throughout the genome to investigate the presence of aneuploidy (abnormal chromosomal counts) in samples from cancer patients (see Appendix E for details). The raw amplicon counts are then used with no further pre-processing. We have two tasks of interest: classification on the basis of either sex or age.

For each of the above described problems, we first compute an embedding matrix to project the training data using `LOL`, `PCA`, `rrLDA`, and `RP`, and then train `LDA` to classify the resulting low-dimensional representations. The *held-out* set is then projected and classified using the embedding matrix and trained classifier respectively, and the average cross-validated error is computed over all folds of the data. For each problem, the optimal dimensionality for each strategy is selected to be the number of embedding dimensions with the lowest average cross-validated error. We compute Cohen’s Kappa κ to compare performance across methods because it normalizes the performance of the classification strategy between zero (the classifier is equivalent to the *random chance* classifier) and one (the classifier performs perfectly). Finally, for each projection technique, we measure the effect size for each strategy as the difference $\kappa(\text{PCA}) - \kappa(\text{embed})$. See Appendix E for a table detailing the datasets employed.

Our `FlashLOL` implementations are the only algorithms that could successfully run on these data with a single core on a standard desktop computer. In Figure 5(A), `LOL` is the only technique to outperform `PCA` on all problems. Figure 5(B) shows the relative ranks of the average cross-validated misclassification rates for the `LDA` classifier on each dataset after projection with the specified embedding technique. For all problems, `LOL` is the technique with the lowest average cross-validated misclassification rate. Further, `LOL` performs significantly better than all other techniques (Wilcoxon signed-rank statistic, all p -values = 0.008). The average misclassification rate achieved at the optimal number of embedding dimensions via `LOL` is between 5% and 15% across all datasets, which is the same performance we and others obtain using extensively processed and downsampled data that is typically required on similar datasets [32, 71]. `LOL` therefore enables researchers to side-step hotly debated pre-processing issues by hardly pre-processing at all, and instead simply applying `LOL` to the data in its native dimensionality.

Discussion

We have introduced a very simple methodology to improve performance on supervised learning problems with wide data (that is, big data where dimensionality is at least as large as sample size) by using class-conditional moments to estimate a low rank projection under a generalized framework, `XOX`. In particular, `LOL` uses both the difference of the means and the class-centered covariance matrices, which enables it to outperform `PCA`, as well as existing supervised linear classification schemes, in a wide variety of scenarios without incurring any meaningful additional computational cost. Straight-forward generalizations enable robust and nonlinear variants by using robust estimators and/or class specific covariance estimators. Our open source implementation optimally scales to terabyte datasets. Moreover, the intuition can be extended for both hypothesis testing and regression (see Appendix F for additional numerical examples in these settings).

Two commonly applied approaches in these settings are partial least squares (`PLS`) and canonical correlation analysis (`CCA`). `CCA` is equivalent to `rrLDA` whenever $p < n$, which is not of interest here. When $p \geq n$, `CCA` and `rrLDA` are not equivalent; however, in such settings, `CCA` exhibits the “maximal data piling problem” [5] (see Appendix B.VI for details). Specifically, all the points in each class are projected onto the exact same point. This results in severe overfitting of the data, yielding poor empirical

performance in essentially all settings we considered here (the first dimension of *CCA* is typically worse even than the difference of the means). While *PLS* does not exhibit these problems, it lacks strong theoretical guarantees and simple geometric intuition. In contrast to *XOX*, neither *CCA* nor *PLS* enable straightforward generalizations, such as when there are outliers or the discriminant boundary is quadratic (see Figure 3). Further, across all simulations, *XOX* outperforms both of these approaches, sometimes quite dramatically (for example, *XOX* outperforms *CCA* on over all of the simulations considered). Finally, no scalable nor parallelized implementations are readily available for these methods (see Figure 4). One could use stochastic gradient descent with penalties to solve these other optimization problems, but they would still need to tune the penalty parameter which would be quite computationally costly. Neither *PLS* nor *CCA* could be successfully run on the massive neuroimaging dataset nor the amplicon-level genomics dataset using readily-available tools.

Many previous investigations have addressed similar challenges. The celebrated Fisherfaces paper was the first to compose Fisher’s *LDA* with *PCA* (equivalent to *PCA* in this manuscript) [10]. The authors showed via a sequence of numerical experiments the utility of projecting the data using *PCA* prior to classifying with *LDA*. We extend this work by adding a supervised component to the initial projection. Moreover, we provide the geometric intuition for why and when incorporating supervision is advantageous, with numerous examples demonstrating its superiority, and theoretical guarantees formalizing when *LOL* outperforms *PCA*. The “sufficient dimensionality reduction” literature has similar insights, but a different construction that typically requires the dimensionality to be smaller than the sample size [25, 36, 37, 55, 69] (although see [26] for some promising work). More recently, communication-inspired classification approaches have yielded theoretical bounds on linear and affine classification performance [62]; they do not, however, explicitly compare different projections, and the bounds we provide are more general and tighter. Moreover, none of the above strategies have implementations that scale to millions or billions of features. Recent big data packages are designed for millions or billions of samples [3, 4]. In biomedical sciences, however, it is far more common to have tens or hundreds of samples, and millions or billions of features (e.g., genomics or connectomics).

Most manifold learning methods, while exhibiting both strong theoretical [6, 29, 33] and empirical performance, are typically fully unsupervised. Thus, in classification problems, they discover a low-dimensional representation of the data, ignoring the labels. This approach can be highly problematic when the discriminant dimensions and the directions of maximal variance in the learned manifold are not aligned (see Figure 1 for some examples). Moreover, nonlinear manifold learning techniques tend to learn a mapping from the original samples to a low-dimensional space, but do not learn a projection, meaning that new samples cannot easily be mapped onto the low-dimensional space, a requirement for supervised learning. Deep learning methods [38] can easily be supervised, but they tend to require huge sample sizes, lack theoretical guarantees, or are opaque “black-boxes” that are insufficient for many biomedical applications. This yields a dearth of “out of the box” supervised scalable dimensionality reduction techniques with strong theoretical guarantees with respect to classification performance bounds designed for wide datasets. Random forests circumvent many of these problems, but implementations that operate on millions of dimensions do not exist [70], and often produce embeddings that perform no better than *PCA* on wide datasets (Figure 5).

Recently discussed strategies have identified techniques for recovering the loading vectors for *PCA* from the weights of a single-layer auto-encoder [63]. Similarly, we believe there may be promise in devising a harmony between *LOL* and supervised auto-encoder strategies to identify the spaces spanned by the first and second moments in unison. Successive techniques, such as unsupervised regularization of supervised autoencoders [2] and supervised dictionary learners [1], may show promise for constructive development of the projection matrix through optimization, rather than estimation, techniques. Unfor-

tunately, these approaches lack standard numerical packages for direct comparison, evaluation, and implementation. Future work may seek to highlight the similarities, or differences, possible through such techniques.

Other approaches formulate an optimization problem, such as projection pursuit [46] and empirical risk minimization [11]. These methods are limited because they are prone to fall into local minima, require costly iterative algorithms, lack any theoretical guarantees on classification accuracy [11]. Feature selection strategies, such as higher criticism thresholding [30] effectively filter the dimensions, possibly prior to performing PCA on the remaining features [8]. These approaches could be combined with LOL in ultrahigh-dimensional problems. Similarly, another recently proposed supervised PCA variant builds on the elegant Hilbert-Schmidt independence criterion [41] to learn an embedding [9]. Our theory demonstrates that under the Gaussian model, composing this linear projection with the difference of the means will improve subsequent performance under general settings, implying that this will be a fertile avenue to pursue. A natural extension to this work would therefore be to estimate a Gaussian mixture model per class, rather than simply a Gaussian per class, and project onto the subspace spanned by the collection of all Gaussians.

In conclusion, the key XOX idea, appending class-conditional moment estimates to convert unsupervised manifold learning to supervised manifold learning, has many potential applications and extensions. We have presented the first few, including LOL, QQQ, and RLOL, which demonstrated the flexibility of XOX under both theoretical and benchmark settings. Incorporating additional nonlinearities via higher order moments, kernel methods [61], ensemble methods [21] such as random forests [15], and multiscale methods [6] are all of immediate interest.

Data Availability Data used within this manuscript are available from <https://neurodata.io/lol/> and <https://neurodata.io/mri>.

Code Availability MATLAB, R, and Python code for the experiments performed in this manuscript and a docker container for FlashLOL are available from <https://neurodata.io/lol/>, and an R package is available on the Comprehensive R Archive Network (CRAN) [17].

Bibliography

- [1] Sep 2013. URL <https://arxiv.org/abs/1009.5358.pdf>. [Online; accessed 5. Nov. 2020]. 11
- [2] Nov 2020. URL <https://papers.nips.cc/paper/2018/file/2a38a4a9316c49e5a833517c45d31070-Paper.pdf>. [Online; accessed 5. Nov. 2020]. 11
- [3] Martín Abadi, Ashish Agarwal, Paul Barham, Eugene Brevdo, Zhifeng Chen, Craig Citro, Greg S Corrado, Andy Davis, Jeffrey Dean, Matthieu Devin, et al. Tensorflow: Large-scale machine learning on heterogeneous distributed systems. *arXiv preprint arXiv:1603.04467*, 2016. 11
- [4] Alekh Agarwal, Oliveier Chapelle, Miroslav Dudík, and John Langford. A reliable effective terascale linear learning system. *J. Mach. Learn. Res.*, 15:1111–1133, 2014. 11
- [5] J. Ahn and J. S. Marron. The maximum data piling direction for discrimination. *Biometrika*, 97: 254–259, 2010. 10, 26
- [6] William K. Allard, Guangliang Chen, and Mauro Maggioni. Multi-scale geometric methods for data sets II: Geometric Multi-Resolution Analysis. *Applied and Computational Harmonic Analysis*, 32(3):435–462, May 2012. ISSN 10635203. doi: 10.1016/j.acha.2011.08.001. URL <http://linkinghub.elsevier.com/retrieve/pii/S1063520311000868>. 11, 12
- [7] E. Anderson, Z. Bai, C. Bischof, S. Blackford, J. Demmel, J. Dongarra, J. Du Croz, A. Greenbaum, S. Hammerling, A. McKenney, and D. Sorensen. *LAPACK Users' Guide: Third Edition*. SIAM, 1999. ISBN 0898714478. URL <https://books.google.com/books?hl=en&lr=&id=AZlvEnr9gCgC&pgis=1>. 23
- [8] Eric Bair, Trevor Hastie, Debashis Paul, and Robert Tibshirani. Prediction by supervised principal components. *J. Am. Stat. Assoc.*, 101(473):119–137, mar 2006. 12
- [9] Elnaz Barshan, Ali Ghodsi, Zohreh Azimifar, and Mansoor Zolghadri Jahromi. Supervised principal component analysis: Visualization, classification and regression on subspaces and submanifolds. *Pattern Recognit.*, 44(7):1357–1371, jul 2011. 12
- [10] Peter N. Belhumeur, João P. Hespanha, and David J. Kriegman. Eigenfaces vs. fisherfaces: Recognition using class specific linear projection. *IEEE Transactions on Pattern Analysis and Machine Intelligence*, 19(7):711–720, 1997. ISSN 01628828. 11
- [11] Mikhail Belkin, Partha Niyogi, and Vikas Sindhwani. Manifold Regularization: A Geometric Framework for Learning from Labeled and Unlabeled Examples. *The Journal of Machine Learning Research*, 7:2399–2434, December 2006. ISSN 15324435. doi: 10.1016/j.neuropsychologia.2009.02.028. URL <http://dl.acm.org/citation.cfm?id=1248547.1248632><http://dl.acm.org/citation.cfm?id=1248632>. 12
- [12] Yoshua Bengio, Jean-François Paiement, Pascal Vincent, Olivier Delalleau, Nicolas L Roux, and Marie Ouimet. Out-of-Sample extensions for LLE, isomap, MDS, eigenmaps, and spectral clustering. In S Thrun, L K Saul, and P B Schölkopf, editors, *Advances in Neural Information Processing Systems 16*, pages 177–184. MIT Press, 2004. 3

- [13] Peter J. Bickel and Elizaveta Levina. Some theory for Fisher’s linear discriminant function, ‘naive Bayes’, and some alternatives when there are many more variables than observations. *Bernoulli*, 10(6):989–1010, December 2004. ISSN 1350-7265. URL <http://projecteuclid.org/euclid.bj/1106314847>. 4
- [14] L. Breiman. Statistical modeling: The two cultures. *Statistical Science*, 16(3):199–231, 2001. 24
- [15] Leo Breiman. Random forests. *Machine learning*, 45(1):5–32, 2001. 12
- [16] Richard G Brereton and Gavin R Lloyd. Partial least squares discriminant analysis: taking the magic away: PLS-DA: taking the magic away. *J. Chemom.*, 28(4):213–225, April 2014. 2
- [17] Eric W Bridgeford, Minh Tang, Jason Yim, and Joshua T Vogelstein. Linear optimal Low-Rank projection, May 2018. 12
- [18] Eric W. Bridgeford, Shangsi Wang, Zhi Yang, Zeyi Wang, Ting Xu, Cameron Craddock, Jayanta Dey, Gregory Kiar, William Gray-Roncal, Carlo Colantuoni, Christopher Douville, Stephanie Noble, Carey E. Priebe, Brian Caffo, Michael Milham, Xi-Nian Zuo, and Joshua T. Vogelstein. Eliminating accidental deviations to minimize generalization error and maximize reliability: applications in connectomics and genomics. *bioRxiv*, 2020. doi: 10.1101/802629. URL <https://www.biorxiv.org/content/early/2020/01/18/802629>. 9
- [19] Tony Cai, Zongming Ma, and Yihong Wu. Optimal estimation and rank detection for sparse spiked covariance matrices. *Probab. Theory Related Fields*, 161(3-4):781–815, apr 2015. 35
- [20] Emmanuel J. Candès and Terence Tao. Near-Optimal Signal Recovery From Random Projections: Universal Encoding Strategies? *IEEE Transactions on Information Theory*, 52(12):5406–5425, dec 2006. ISSN 0018-9448. doi: 10.1109/TIT.2006.885507. URL <http://ieeexplore.ieee.org/lpdocs/epic03/wrapper.htm?arnumber=4016283>. 8
- [21] Timothy I Cannings and Richard J Samworth. Random-projection ensemble classification. *arXiv*, Apr 2015. 12
- [22] William R. Carson, Minhua Chen, Miguel R. D. Rodrigues, Robert Calderbank, and Lawrence Carin. Communications-Inspired Projection Design with Application to Compressive Sensing. *arXiv*, Jun 2012. doi: 10.1137/120878380. 21
- [23] H. Chernoff. A measure of asymptotic efficiency for tests of a hypothesis based on the sum of observations. *Annals of Mathematical Statistics*, 23:493–507, 1952. 6, 29
- [24] Jacob Cohen. A coefficient of agreement for nominal scales. *Educational and Psychological Measurement*, 20(1):37–46, 1960. doi: 10.1177/001316446002000104. URL <https://doi.org/10.1177/001316446002000104>. 36
- [25] R. Dennis Cook and Liqiang Ni. Sufficient Dimension Reduction via Inverse Regression. *Journal of the American Statistical Association*, 100(470):410–428, June 2005. ISSN 0162-1459. doi: 10.1198/016214504000001501. URL <http://amstat.tandfonline.com/doi/abs/10.1198/016214504000001501#.U6tH3Y1dUts>. 11
- [26] R. Dennis Cook, Liliana Forzani, and Adam J. Rothman. Prediction in abundant high-dimensional linear regression. *Electronic Journal of Statistics*, 7:3059–3088, 2013. URL <https://projecteuclid.org/euclid.ejs/1387207935>. 11

- [27] cran. robust, Oct 2020. URL <https://github.com/cran/robust>. [Online; accessed 15. Oct. 2020]. 6
- [28] I. Csizár. Information-type measures of difference of probability distributions and indirect observations. *Studia Scientiarum Mathematicarum Hungarica*, 2:229–318, 1967. 29
- [29] V de Silva and Joshua B Tenenbaum. Global Versus Local Methods in Nonlinear Dimensionality Reduction. In *Neural Information Processing Systems*, pages 721–728, 2003. 11
- [30] David L. Donoho and Jiashun Jin. Higher criticism thresholding: Optimal feature selection when useful features are rare and weak. *Proceedings of the National Academy of Sciences of the United States of America*, 105(39):14790–5, September 2008. ISSN 1091-6490. doi: 10.1073/pnas.0807471105. URL <http://www.pnas.org/content/105/39/14790><http://www.pnas.org/content/105/39/14790.short>. 12
- [31] Christopher Douville, Joshua D. Cohen, Janine Ptak, Maria Popoli, Joy Schaefer, Natalie Silliman, Lisa Dobbyn, Robert E. Schoen, Jeanne Tie, Peter Gibbs, Michael Goggins, Christopher L. Wolfgang, Tian-Li Wang, Ie-Ming Shih, Rachel Karchin, Anne Marie Lennon, Ralph H. Hruban, Cristian Tomasetti, Chetan Bettegowda, Kenneth W. Kinzler, Nickolas Papadopoulos, and Bert Vogelstein. Assessing aneuploidy with repetitive element sequencing. *Proc. Natl. Acad. Sci. U.S.A.*, 117(9): 4858–4863, Mar 2020. ISSN 0027-8424. doi: 10.1073/pnas.1910041117. 10, 37
- [32] J M Duarte-Carvajalino and Neda Jahanshad. Hierarchical topological network analysis of anatomical human brain connectivity and differences related to sex and kinship. *Neuroimage*, 59(4): 3784–3804, 2011. 10
- [33] Carl Eckart and Gale Young. The approximation of one matrix by another of lower rank. *Psychometrika*, 1(3):211–218, September 1936. ISSN 0033-3123. doi: 10.1007/BF02288367. URL <http://www.springerlink.com/content/9v4274h33h751q24/>. 11
- [34] Jianqing Fan, Yang Feng, and Xin Tong. A road to classification in high dimensional space: the regularized optimal affine discriminant. *Journal of the Royal Statistical Society: Series B (Statistical Methodology)*, 74(4):745–771, September 2012. ISSN 13697412. doi: 10.1111/j.1467-9868.2012.01029.x. URL <http://doi.wiley.com/10.1111/j.1467-9868.2012.01029.x>. 2, 4, 21
- [35] R. A. Fisher. Theory of Statistical Estimation. *Mathematical Proceedings of the Cambridge Philosophical Society*, 22(05):700–725, October 1925. ISSN 0305-0041. doi: 10.1017/S0305004100009580. URL http://journals.cambridge.org/abstract_S0305004100009580. 1
- [36] Kenji Fukumizu, Francis R Bach, and Michael I. Jordan. Dimensionality Reduction for Supervised Learning with Reproducing Kernel Hilbert Spaces. *Journal of Machine Learning Research*, 5: 73–99, 2004. 11
- [37] Amir Globerson and Naftali Tishby. Sufficient Dimensionality Reduction. *Journal of Machine Learning Research*, 3(7-8):1307–1331, October 2003. ISSN 1532-4435. doi: 10.1162/153244303322753689. URL http://www.crossref.org/jmlr_DOI.html. 11
- [38] Ian Goodfellow, Yoshua Bengio, Aaron Courville, and Yoshua Bengio. *Deep learning*, volume 1. MIT press Cambridge, 2016. 2, 11

- [39] William R Gray, John A Bogovic, Joshua T Vogelstein, Bennett A Landman, Jerry L Prince, and R Jacob Vogelstein. Magnetic resonance connectome automated pipeline. *IEEE Pulse*, 3(2): 42–48, 2011. 9
- [40] William Gray Roncal et al. MIGRAINE: MRI Graph Reliability Analysis and Inference for Connectomics. *Global Conference on Signal and Information Processing*, 2013. 9
- [41] A. Gretton, R. Herbrich, A. Smola, O. Bousquet, and B. Scholkopf. Kernel methods for measuring independence. *Journal of Machine Learning Research*, 6:2075–2129, 2005. 12
- [42] Trevor Hastie and Robert Tibshirani. Discriminant analysis by gaussian mixtures. *J. R. Stat. Soc. Series B Stat. Methodol.*, 58(1):155–176, 1996. 4
- [43] Trevor Hastie, Robert Tibshirani, and Jerome H. Friedman. The Elements of Statistical Learning: Data Mining, Inference, and Prediction. *BeiJing: Publishing House of Electronics Industry*, 2004. 6
- [44] Trevor Hastie, Kenneth Ward Church, Ping Li, and Kenneth Church Kdd. Very sparse random projections. *Proceedings of the 12th ACM SIGKDD international conference on Knowledge discovery and data mining - KDD '06*, page 287, 2006. doi: 10.1145/1150402.1150436. URL <http://portal.acm.org/citation.cfm?doid=1150402.1150436>. 8
- [45] Trevor Hastie, Robert Tibshirani, and Martin Wainwright. *Statistical Learning with Sparsity: The Lasso and Generalizations (Chapman & Hall/CRC Monographs on Statistics & Applied Probability)*. Chapman and Hall/CRC, 1 edition edition, may 2015. 2
- [46] Peter J. Huber. Projection Pursuit. *The Annals of Statistics*, 13(2):435–475, June 1985. ISSN 2168-8966. URL <http://projecteuclid.org/euclid.aos/1176349519>. 12
- [47] Mark Jenkinson et al. FSL. *NeuroImage*, 62(2):782–90, aug 2012. ISSN 1095-9572. URL <http://www.ncbi.nlm.nih.gov/pubmed/21979382>. 37
- [48] I T Jolliffe. Principal component analysis and factor analysis. In *Principal Component Analysis*, Springer Series in Statistics, pages 115–128. Springer, New York, NY, 1986. 1
- [49] Gregory Kiar, Krzysztof J. Gorgolewski, Dean Kleissas, William Gray Roncal, Brian Litt, Brian Wandell, Russel A. Poldrack, Martin Wiener, R. Jacob Vogelstein, Randal Burns, and Joshua T. Vogelstein. Science in the cloud (sic): A use case in mri connectomics. *GigaScience*, gix013, mar 2017. doi: 10.1093/gigascience/gix013. 9
- [50] Alex Krizhevsky, Ilya Sutskever, and Geoffrey E. Hinton. ImageNet Classification with Deep Convolutional Neural Networks. In *Advances in Neural Information Processing Systems*, pages 1097–1105, 2012. URL <http://papers.nips.cc/paper/4824-imagenet-classification-w>. 1
- [51] Bennett A Landman, Alan J Huang, Aliya Gifford, Deepti S Vikram, Issel Anne L Lim, Jonathan A D Farrell, John A Bogovic, Jun Hua, Min Chen, Samson Jarso, Seth A Smith, Suresh Joel, Susumu Mori, James J Pekar, Peter B Barker, Jerry L Prince, and Peter C M van Zijl. Multi-parametric neuroimaging reproducibility: a 3-T resource study. *Neuroimage*, 54(4):2854–2866, February 2011. 37
- [52] C. C. Leang and D. H. Johnson. On the asymptotics of M-hypothesis bayesian detection. *IEEE Transactions on Information Theory*, 43:280–282, 1997. 30

- [53] Yann LeCun, Corinna Cortes, and Chris Burges. MNIST handwritten digit database. URL <http://yann.lecun.com/exdb/mnist/>. 2
- [54] John A Lee and Michel Verleysen. *Nonlinear Dimensionality Reduction (Information Science and Statistics)*. Springer, 2007 edition edition, December 2007. 2
- [55] Ker-Chau Li. Sliced Inverse Regression for Dimension Reduction. *Journal of the American Statistical Association*, 86(414):316–327, June 1991. ISSN 0162-1459. doi: 10.1080/01621459.1991.10475035. URL <http://www.tandfonline.com/doi/abs/10.1080/01621459.1991.10475035>. 11
- [56] Miles Lopes, Laurent Jacob, and Martin J. Wainwright. A More Powerful Two-Sample Test in High Dimensions using Random Projection. In *Neural Information Processing Systems*, pages 1206–1214, 2011. URL <http://papers.nips.cc/paper/4260-a-more-powerful-two-sample-test-in-high-dimensions-using-random-projection>. 38, 39
- [57] Qing Mai, Hui Zou, and Ming Yuan. A direct approach to sparse discriminant analysis in ultra-high dimensions. *Biometrika*, 99(1), Feb 2012. doi: 10.2307/41720670. 21
- [58] Julien Mairal, Jean Ponce, Guillermo Sapiro, Andrew Zisserman, and Francis R. Bach. Supervised Dictionary Learning. In *Advances in Neural Information Processing Systems*, pages 1033–1040, 2009. URL <http://papers.nips.cc/paper/3448-supervised>. 8
- [59] K. V. Mardia, J. T. Kent, and J. M. Bibby. *Multivariate Analysis*. Academic Press, 1979. 26
- [60] John Mazziotta et al. A four-dimensional probabilistic atlas of the human brain. *Journal of the American Medical Informatics Association*, 8(5):401–430, 2001. 37
- [61] S. Mika, G. Ratsch, J. Weston, B. Scholkopf, and K.R. Mullers. Fisher discriminant analysis with kernels. In *Neural Networks for Signal Processing IX: Proceedings of the 1999 IEEE Signal Processing Society Workshop (Cat. No.98TH8468)*, pages 41–48. IEEE, 1999. ISBN 0-7803-5673-X. doi: 10.1109/NNSP.1999.788121. URL <http://ieeexplore.ieee.org/lpdocs/epic03/wrapper.htm?arnumber=788121>. 12
- [62] M Nokleby, M Rodrigues, and R Calderbank. Discrimination on the grassmann manifold: Fundamental limits of subspace classifiers. *IEEE Trans. Inf. Theory*, 61(4):2133–2147, April 2015. 11
- [63] Elad Plaut. From Principal Subspaces to Principal Components with Linear Autoencoders. *arXiv*, Apr 2018. URL <https://arxiv.org/abs/1804.10253v3>. 11
- [64] H. Shin and R. L. Eubank. Unit canonical correlations and high-dimensional discriminant analysis. *Journal of Statistical Computation and Simulation*, 81:167–178, 2011. 2, 26
- [65] Stephen M Smith et al. Advances in functional and structural MR image analysis and implementation as FSL. *NeuroImage*, 23 Suppl 1:S208–19, jan 2004. ISSN 1053-8119. URL <http://www.ncbi.nlm.nih.gov/pubmed/15501092>. 37
- [66] Weijie Su, Malgorzata Bogdan, and Emmanuel Candes. False discoveries occur early on the lasso path. *arXiv*, nov 2015. 2

- [67] Cajo J F ter Braak and Sijmen de Jong. The objective function of partial least squares regression, 1998. [2](#)
- [68] Robert Tibshirani. Regression Shrinkage and Selection via the Lasso. *Journal of the Royal Statistical Society. Series B*, 58:267–288, 1996. [2](#)
- [69] Naftali Tishby, Fernando C Pereira, and William Bialek. The information bottleneck method arXiv : physics / 0004057v1 [physics . data-an] 24 Apr 2000. *Neural Computation*, pages 1–16, 1999. [11](#)
- [70] T Tomita, M Maggioni, and J Vogelstein. ROFLMAO: Robust oblique forests with linear MAtrix operations. In *Proceedings of the 2017 SIAM International Conference on Data Mining*, Proceedings, pages 498–506. Society for Industrial and Applied Mathematics, June 2017. [11](#)
- [71] J T Vogelstein, W G Roncal, R J Vogelstein, and C E Priebe. Graph classification using Signal-Subgraphs: Applications in statistical connectomics. *IEEE Trans. Pattern Anal. Mach. Intell.*, 35(7):1539–1551, 2013. [10](#)
- [72] J. T. Vogelstein, Y. Park, T. Ohyama, R. Kerr, J. Truman, C. E. Priebe, and M. Zlatic. Discovery of brainwide neural-behavioral maps via multiscale unsupervised structure learning. *Science*, 344(6182):386–392, 2014. [1](#)
- [73] Daniela M. Witten and Robert Tibshirani. Covariance-regularized regression and classification for high-dimensional problems. *Journal of the Royal Statistical Society. Series B, Statistical methodology*, 71(3):615–636, February 2009. ISSN 1369-7412. doi: 10.1111/j.1467-9868.2009.00699.x. URL <http://www.pubmedcentral.nih.gov/articlerender.fcgi?artid=2806603&tool=pmcentrez&rendertype=abstract>. [2](#)
- [74] Mark W Woolrich et al. Bayesian analysis of neuroimaging data in FSL. *NeuroImage*, 45(1 Suppl): S173–86, mar 2009. ISSN 1095-9572. URL <http://www.sciencedirect.com/science/article/pii/S1053811908012044>. [37](#)
- [75] Da Zheng, Disa Mhembere, Randal Burns, Joshua Vogelstein, Carey E. Priebe, and Alexander S. Szalay. FlashGraph: Processing billion-node graphs on an array of commodity SSDs. In *13th USENIX Conference on File and Storage Technologies (FAST 15)*, Santa Clara, CA, 2015. [8](#)
- [76] Da Zheng, Randal Burns, Joshua Vogelstein, Carey E. Priebe, and Alexander S. Szalay. An ssd-based eigensolver for spectral analysis on billion-node graphs. *CoRR*, abs/1602.01421, 2016.
- [77] Da Zheng, Disa Mhembere, Joshua T Vogelstein, Carey E Priebe, and Randal Burns. Flashmatrix: Parallel, scalable data analysis with generalized matrix operations using commodity ssds. *arXiv preprint arXiv:1604.06414*, 2016. [8](#), [39](#)
- [78] Xi-Nian Zuo, Jeffrey S Anderson, Pierre Bellec, Rasmus M Birn, Bharat B Biswal, Janusch Blautzik, John CS Breitner, Randy L Buckner, Vince D Calhoun, F Xavier Castellanos, et al. An open science resource for establishing reliability and reproducibility in functional connectomics. *Scientific data*, 1:140049, 2014. [9](#), [37](#)

Acknowledgements

The authors are grateful for the support by the XDATA program of the Defense Advanced Research Projects Agency (DARPA) administered through Air Force Research Laboratory contract FA8750-12-2-0303; DARPA GRAPHS contract N66001-14-1-4028; and DARPA SIMPLEX program through SPAWAR contract N66001-15-C-4041, and DARPA Lifelong Learning Machines program through contract FA8650-18-2-7834.

A Theoretical Background

A.I The Classification Problem

Let (X, Y) be a pair of random variables, jointly sampled from $F := F_{X,Y} = F_{X|Y}F_Y$, with density denoted $f_{X,Y}$. Let X be a multivariate vector-valued random variable, such that its realizations live in p dimensional Euclidean space, $\mathbf{x} \in \mathbb{R}^p$. Let Y be a categorical random variable, whose realizations are discrete, $y \in \{0, \dots, C-1\}$. The goal of a classification problem is to find a function $g(\mathbf{x})$ such that its output tends to be the true class label y :

$$g^*(\mathbf{x}) := \operatorname{argmax}_{g \in \mathcal{G}} \mathbb{P}[g(\mathbf{x}) = y].$$

When the joint distribution of the data is known, then the Bayes optimal solution is:

$$g^*(\mathbf{x}) := \operatorname{argmax}_y f_{y,\mathbf{x}} = \operatorname{argmax}_y f_{\mathbf{x}|y}f_y = \operatorname{argmax}_y \{\log f_{\mathbf{x}|y} + \log f_y\} \quad (1)$$

Denote expected misclassification rate of classifier g for a given joint distribution F ,

$$L_g^F := \mathbb{E}[g(\mathbf{x}) \neq y] := \int \mathbb{P}[g(\mathbf{x}) \neq y] f_{\mathbf{x},y} d\mathbf{x} dy,$$

where \mathbb{E} is the expectation, which in this case, is with respect to $F_{X,Y}$. For brevity, we often simply write L_g , and we define $L_* := L_{g^*}$.

A.II Linear Discriminant Analysis (LDA)

Linear Discriminant Analysis (LDA) is an approach to classification that uses a linear function of the first two moments of the distribution of the data. More specifically, let $\boldsymbol{\mu}_j = \mathbb{E}[F_{X|Y=j}]$ denote the class conditional mean, and let $\boldsymbol{\Sigma} = \mathbb{E}[F_X^2]$ denote the joint covariance matrix, and the class priors are $\pi_j = \mathbb{P}[Y = j]$. Using this notation, we can define the LDA classifier:

$$g_{\text{LDA}}(\mathbf{x}) := \operatorname{argmin}_y \left[\frac{1}{2}(\mathbf{x} - \boldsymbol{\mu}_y)^\top \boldsymbol{\Sigma}^{-1}(\mathbf{x} - \boldsymbol{\mu}_y) - \log \pi_y \right],$$

Let L_{LDA}^F be the expected misclassification rate of the above classifier for distribution F . Assuming equal class prior and centered means, re-arranging a bit, we obtain

$$g_{\text{LDA}}(\mathbf{x}) := \operatorname{argmin}_y \mathbf{x}^\top \boldsymbol{\Sigma}^{-1} \boldsymbol{\mu}_y.$$

In words, the LDA classifier chooses the class that maximizes the magnitude of the projection of an input vector \mathbf{x} onto $\boldsymbol{\Sigma}^{-1} \boldsymbol{\mu}_y$. When there are only two classes, letting $\boldsymbol{\delta} = \boldsymbol{\mu}_0 - \boldsymbol{\mu}_1$, the above further simplifies to

$$g_{2\text{LDA}}(\mathbf{x}) := \mathbb{I}\{\mathbf{x}^\top \boldsymbol{\Sigma}^{-1} \boldsymbol{\delta} > 0\}.$$

Note that the equal class prior and centered means assumptions merely changes the threshold constant from 0 to some other constant.

A.III LDA Model

A statistical model is a family of distributions indexed by a parameter $\theta \in \Theta$, $\mathcal{F}_\theta = \{F_\theta : \theta \in \Theta\}$. Consider the special case of the above where $F_{\mathbf{X}|Y=y}$ is a multivariate Gaussian distribution, $\mathcal{N}(\boldsymbol{\mu}_y, \boldsymbol{\Sigma})$, where each class has its own mean, but all classes have the same covariance. We refer to this model as the LDA model. Let $\theta = (\boldsymbol{\pi}, \boldsymbol{\mu}, \boldsymbol{\Sigma})$, and let $\Theta_{C\text{-LDA}} = (\Delta_C, \mathbb{R}^{p \times C}, \mathbb{R}_{>0}^{p \times p})$, where $\boldsymbol{\mu} = (\boldsymbol{\mu}_1, \dots, \boldsymbol{\mu}_C)$, Δ_C is the C dimensional simplex, that is $\Delta_C = \{\mathbf{x} : x_i \geq 0 \forall i, \sum_i x_i = 1\}$, and $\mathbb{R}_{>0}^{p \times p}$ is the set of positive definite $p \times p$ matrices. Denote $\mathcal{F}_{\text{LDA}} = \{F_\theta : \theta \in \Theta_{\text{LDA}}\}$. The following lemma is well known [22]:

Lemma 1. $L_{\text{LDA}}^F = L_*^F$ for any $F \in \mathcal{F}_{\text{LDA}}$.

B Formal Definition of LOL and Related Projection Based Classifiers

Let $\mathbf{A} \in \mathbb{R}^{d \times p}$ be a ‘‘projection matrix’’, that is, a matrix that projects p -dimensional data into a d -dimensional subspace. The question that motivated this work is: what is the best projection matrix that we can estimate, to use to ‘‘pre-process’’ the data prior to classifying the data? Projecting the data \mathbf{x} onto a low-dimensional subspace, and then classifying via LDA in that subspace is equivalent to redefining the parameters in the low-dimensional subspace, $\boldsymbol{\Sigma}_A = \mathbf{A}\boldsymbol{\Sigma}\mathbf{A}^\top \in \mathbb{R}^{d \times d}$ and $\boldsymbol{\delta}_A = \mathbf{A}\boldsymbol{\delta} \in \mathbb{R}^d$, and then using g_{LDA} in the low-dimensional space. When $C = 2$, $\pi_0 = \pi_1$, and $(\boldsymbol{\mu}_0 + \boldsymbol{\mu}_1)/2 = \mathbf{0}$, this amounts to:

$$g_A^d(\mathbf{x}) := \mathbb{I}\{(\mathbf{A}\mathbf{x})^\top \boldsymbol{\Sigma}_A^{-1} \boldsymbol{\delta}_A > 0\}, \text{ where } \mathbf{A} \in \mathbb{R}^{d \times p}. \quad (2)$$

Let $L_A^d := \int \mathbb{P}[g_A^d(\mathbf{x}) = y] f_{\mathbf{x},y} d\mathbf{x} dy$. Our goal therefore is to be able to choose A for a given parameter setting $\theta = (\boldsymbol{\pi}, \boldsymbol{\delta}, \boldsymbol{\Sigma})$, such that L_A is as small as possible (note that L_A will never be smaller than L_*).

In the naive case where $(\boldsymbol{\Sigma}_A, \boldsymbol{\delta}_A)$ are known, we seek to solve the following linear optimization problem:

$$\begin{aligned} & \underset{\mathbf{A}}{\text{minimize}} && \mathbb{E}[\mathbb{I}\{\mathbf{x}^\top \mathbf{A}^\top \boldsymbol{\Sigma}_A^{-1} \boldsymbol{\delta}_A > 0\} \neq y] \\ & \text{subject to} && \mathbf{A} \in \mathbb{R}^{d \times p}. \end{aligned} \quad (3)$$

When $(\boldsymbol{\Sigma}_A, \boldsymbol{\delta}_A)$ are not known, however, the optimization problem becomes non-convex. With $\boldsymbol{\Sigma}_A$ and $\boldsymbol{\delta}_A$ as above:

$$\begin{aligned} & \underset{\mathbf{A}, \boldsymbol{\Sigma}, \boldsymbol{\delta}}{\text{minimize}} && \mathbb{E}[\mathbb{I}\{\mathbf{x}^\top \mathbf{A}^\top \boldsymbol{\Sigma}_A^{-1} \boldsymbol{\delta}_A > 0\} \neq y] \\ & \text{subject to} && \mathbf{A} \in \mathbb{R}^{d \times p}. \end{aligned} \quad (4)$$

While there are numerous approaches to solve related convex optimization problems through various sets of assumptions [34, 57], we do not consider such techniques in this manuscript theoretically. This is because assuming either a structure for $\boldsymbol{\Sigma}_A$ or $\boldsymbol{\delta}_A$ presupposes an understanding of the properties of the feature space for wide data, which is often unsuitable if the dataset is large or has considerable complexity.

Let $\mathcal{A} = \{\mathbf{A} : \mathbf{A} \in \mathbb{R}^{k \times p}, k \leq p\}$, $\mathcal{A}^d = \{\mathbf{A} : \mathbf{A} \in \mathbb{R}^{d \times p}\}$, and let $\mathcal{A}_* \subset \mathcal{A}$ be the set of \mathbf{A} that minimizes Eq. (4), and let $\mathbf{A}_* \in \mathcal{A}_*$. Let $L_{\mathbf{A}}^* = L_{\mathbf{A}_*}$ be the misclassification rate for any $\mathbf{A} \in \mathcal{A}_*$, that is, $L_{\mathbf{A}}^*$ is the Bayes optimal misclassification rate for the classifier that composes \mathbf{A} with LDA.

In our opinion, Eq. (4) is the simplest supervised manifold learning problem there is: a two-class classification problem, where the data are multivariate Gaussians with shared, unknown covariances, the

manifold is linear, and the classification is done via LDA. Nonetheless, solving Eq. (4) is difficult, because we do not know how to evaluate the integral analytically, and we do not know any algorithms that are guaranteed to find the global optimum in finite time. We proceed by studying a few natural choices for A .

B.I Bayes Optimal Projection

Lemma 2. $\delta^\top \Sigma^{-1} \in \mathcal{A}_*$

Proof. Let $B = (\Sigma^{-1} \delta)^\top = \delta^\top (\Sigma^{-1})^\top = \delta^\top \Sigma^{-1}$, so that $B^\top = \Sigma^{-1} \delta$, and plugging this in to Eq. (2). By the above, and noting the symmetry and invertibility of Σ :

$$\begin{aligned}\Sigma_B &= B \Sigma B^\top = \delta^\top \Sigma^{-1} \Sigma (\delta^\top \Sigma^{-1})^\top \\ &= \delta^\top \Sigma^{-1} \Sigma \Sigma^{-1} \delta = \delta^\top \Sigma^{-1} \delta \\ \Rightarrow \Sigma_B^{-1} &= \delta^{-1} \Sigma \delta^{\top -1} \\ \delta_B &= B \delta = \delta^\top \Sigma^{-1} \delta\end{aligned}$$

We obtain:

$$\begin{aligned}g_B(x) &= \mathbb{I}\{x^\top B^\top \Sigma_B^{-1} \delta_B > 0\} \\ &= \mathbb{I}\{x^\top (\Sigma^{-1} \delta) (\Sigma_B^{-1} \delta_B) > 0\} && \text{plugging in } B \\ &= \mathbb{I}\{x^\top (\Sigma^{-1} \delta) (\delta^{-1} \Sigma \delta^{\top -1} \delta^\top \Sigma^{-1} \delta) > 0\} && \text{plug in } \Sigma_B, \delta_B \text{ from above} \\ &= \mathbb{I}\{x^\top \Sigma^{-1} \delta > 0\}\end{aligned}$$

In other words, letting B be the Bayes optimal projection recovers the Bayes classifier, as it should. Or, more formally, for any $F \in \mathcal{F}_{\text{LDA}}$, $L_{\delta^\top \Sigma^{-1}} = L_*$. \square

B.II Principle Components Analysis (PCA) Projection

Principle Components Analysis (PCA) finds the directions of maximal variance in a dataset. PCA is closely related to eigendecompositions and singular value decompositions (SVD). In particular, the top left singular vector of a matrix $X \in \mathbb{R}^{p \times n}$, whose columns are centered, is the eigenvector with the largest eigenvalue of the centered covariance matrix XX^\top . SVD enables one to estimate this eigenvector without ever forming the outer product matrix, because SVD factorizes a matrix X into USV^\top , where U and V are orthonormal $p \times p$ and $n \times n$ matrices, and S is a diagonal matrix, whose diagonal values are decreasing, $s_1 \geq s_2 \geq \dots > s_n$. Defining $U = [\mathbf{u}_1, \mathbf{u}_2, \dots, \mathbf{u}_p]$, where each $\mathbf{u}_i \in \mathbb{R}^p$, then \mathbf{u}_i is the i^{th} eigenvector, and s_i is the square root of the i^{th} eigenvalue of XX^\top . Let $A_d^{\text{PCA}} = [\mathbf{u}_1, \dots, \mathbf{u}_d]$ be the truncated PCA orthonormal matrix, and let $I_{d \times p}$ denote a $d \times p$ dimensional identity matrix.

The PCA matrix is perhaps the most obvious choice of an orthonormal matrix for several reasons. First, truncated PCA minimizes the squared error loss between the original data matrix and all possible rank d representations:

$$\operatorname{argmin}_{A \in \mathbb{R}^{d \times p}} \|X - A^\top A\|_F^2.$$

Second, the ubiquity of PCA has led to a large number of highly optimized numerical libraries for computing PCA (for example, LAPACK [7]).

In this supervised setting, we consider two different variants of PCA, each based on centering the data differently. For the first one, which we refer to as “pooled PCA” (or just PCA for brevity), we center the data by subtracting the “pooled mean” from each sample, that is, we let $\tilde{x}_i = x - \mu$, where $\mu = \mathbb{E}[x]$. For the second, which we refer to as “class conditional PCA”, we center the data by subtracting the “class-conditional mean” from each sample, that is, we let $\tilde{x}_i = x - \mu_y$, where $\mu_y = \mathbb{E}[x|Y = y]$.

Notationally, let $U_d = [u_1, \dots, u_d] \in \mathbb{R}^{p \times d}$, and note that $U_d^T U_d = I_{d \times d}$ and $U_d U_d^T = I_{p \times p}$. Similarly, let $USU^T = \Sigma$, and $US^{-1}U^T = \Sigma^{-1}$. Let S_d be the matrix whose diagonal entries are the eigenvalues, up to the d^{th} one, that is $S_d(i, j) = s_i$ for $i = j \leq d$ and zero otherwise. Similarly, $\Sigma_d = US_dU^T = U_d S_d U_d^T$. Reduced-rank LDA (rrLDA) is a regularized LDA algorithm. Specifically, rather than using the full rank covariance matrix, it uses a rank- d approximation. Formally, let $g_{\text{LDA}} := \mathbb{I}\{x \Sigma^{-1} \delta > 0\}$ be the LDA classifier, and let $g_{\text{rrLDA}}^d := \mathbb{I}\{x \Sigma_d^{-1} \delta > 0\}$ be the regularized LDA classifier, that is, the LDA classifier where the the bottom $p - d$ eigenvalues of the covariance matrix are set to zero.

Lemma 3. *Using class-conditional PCA to pre-process the data, then using LDA on the projected data, is equivalent to rrLDA.*

Proof. Plugging U_d into Eq. (2) for A , and considering only the left side of the operand, we have

$$\begin{aligned}
(Ax)^T \Sigma_A^{-1} \delta_A &= x^T A^T A \Sigma^{-1} A^T A \delta, \\
&= x^T U_d U_d^T \Sigma^{-1} U_d U_d^T \delta, \\
&= x^T U_d U_d^T U S^{-1} U^T U_d U_d^T \delta, \\
&= x^T U_d I_{d \times p} S^{-1} I_{p \times d} U_d^T \delta, \\
&= x^T U_d S_d^{-1} U_d^T \delta, \\
&= x^T \Sigma_d^{-1} \delta.
\end{aligned}$$

□

The implication of this lemma is that if one desires to implement rrLDA, rather than first learning the eigenvectors and then learning LDA, one can instead directly implement regularized LDA by setting the bottom $p - d$ eigenvalues to zero. This latter approach removes the requirement to run SVD twice, therefore reducing the computational burden as well as the possibility of numerical instability issues. We therefore refer to the projection composed of d eigenvectors of the class-conditionally centered covariance matrices, A_{LDA}^d .

B.III Linear Optimal Low-Rank (LOL) Projection

The basic idea of LOL is to use both δ and the top d eigenvectors of the class-conditionally centered covariance. When there are only two classes, $\delta = \mu_0 - \mu_1$. When there are $C > 2$ classes, there are $\binom{C}{2} = \frac{C!}{2(C-2)!}$ pairwise combinations, $\delta_{ij} = \mu_i - \mu_j$ for all $i \neq j$. However, since $\binom{C}{2}$ is nearly C^2 , when C is large, this would mean incorporating many mean difference vectors. Note that $[\delta_{1,2}, \delta_{1,3}, \dots, \delta_{C-1,C}]$ is in fact a rank $C - 1$ matrix, because it is a linear function of the C different means. Therefore, we only need $C - 1$ differences to span the space of all pairwise differences. To

mitigate numerical instability issues, we adopt the following convention. For each class, estimate the expected mean and the number of samples per class, $\boldsymbol{\mu}_c$ and π_c . Sort the means in order of decreasing π_c , so that $\pi_{(1)} > \pi_{(2)} > \dots > \pi_{(C)}$. Then, subtract $\boldsymbol{\mu}_{(1)}$ from all other means: $\boldsymbol{\delta}_i = \boldsymbol{\mu}_{(1)} - \boldsymbol{\mu}_{(i)}$, for $i = 2, \dots, C$. Finally, $\boldsymbol{\delta} = [\boldsymbol{\delta}_2, \dots, \boldsymbol{\delta}_C]$.

Given $\boldsymbol{\delta}$ and $\mathbf{A}_{\text{LDA}}^{d-1}$, to obtain LOL naïvely, we could simply concatenate the two, $\mathbf{A}_{\text{LOL},naive}^d = [\boldsymbol{\delta}, \mathbf{A}_{\text{LDA}}^{d-1}]$. Recall that eigenvectors are orthonormal. To maintain orthonormality between the eigenvectors and vectors of $\boldsymbol{\delta}$, we could easily apply Gram-Schmidt, $\mathbf{A}_{\text{LOL},naive}^d = \text{Orth}([\boldsymbol{\delta}, \mathbf{A}_{\text{LDA}}^{d-1}])$. In practice, this orthogonalization step does not matter much, so we ignore it hereafter. To ensure that $\boldsymbol{\delta}$ and $\boldsymbol{\Sigma}$ are balanced appropriately, we normalize each vector in $\boldsymbol{\delta}$ to have norm unity. Formally, let $\tilde{\boldsymbol{\delta}}_j = \boldsymbol{\delta}_j / \|\boldsymbol{\delta}_j\|$, where $\boldsymbol{\delta}_j$ is the j^{th} difference of the mean vector and let $\mathbf{A}_{\text{LOL}}^d = [\tilde{\boldsymbol{\delta}}, \mathbf{A}_{\text{LDA}}^{d-(C-1)}]$.

When the distribution of the data is not provided, each of the above terms must be estimated from the data. We use the maximum likelihood estimators for each, specifically:

$$n_c = \sum_{i=1}^n \mathbb{I}\{y_i = c\}, \quad (5)$$

$$\hat{\pi}_c = \frac{n_c}{n}, \quad (6)$$

$$\hat{\boldsymbol{\mu}} = \frac{1}{n} \sum_{i=1}^n \mathbf{x}_i, \quad (7)$$

$$\hat{\boldsymbol{\mu}}_c = \frac{1}{n_c} \sum_{i=1}^n \mathbf{x}_i \mathbb{I}\{y_i = c\}. \quad (8)$$

For completeness, below we provide pseudocode for learning the sample version of LOL . The population version does not require the estimation of the parameters.

B.IV rrLDA is rotationally invariant

For certain classification tasks, the observed dimensions (or features) have intrinsic value, e.g. when simple interpretability is desired. However, in many other contexts, interpretability is less important [14]. When the exploitation task at hand is invariant to rotations, then we have no reason to restrict our search space to be sparse in the observed dimensions. For example, we can consider sparsity in the eigenvector basis. Let \mathbf{W} be a rotation matrix, that is $\mathbf{W} \in \mathcal{W} = \{\mathbf{W} : \mathbf{W}^\top = \mathbf{W}^{-1} \text{ and } \det(\mathbf{W}) = 1\}$. Moreover, let $\mathbf{W} \circ F$ denote the distribution F after transformation by an operator \mathbf{W} . For example, if $F = \mathcal{N}(\boldsymbol{\mu}, \boldsymbol{\Sigma})$ then $\mathbf{W} \circ F = \mathcal{N}(\mathbf{W}\boldsymbol{\mu}, \mathbf{W}\boldsymbol{\Sigma}\mathbf{W}^\top)$.

Definition 1. A rotationally invariant classifier has the following property:

$$L_g^F = L_g^{W \circ F}, \quad F \in \mathcal{F} \text{ and } W \in \mathcal{W}.$$

In words, the Bayes risk of using classifier g on distribution F is unchanged if F is first rotated.

Now, we can state the main lemma of this subsection: rrLDA is rotationally invariant.

Lemma 4. $L_{\text{LDA}}^F = L_{\text{LDA}}^{W \circ F}$, for any $F \in \mathcal{F}$.

Proof. rrLDA is in fact simply thresholding $\mathbf{x}^\top \boldsymbol{\Sigma}^{-1} \boldsymbol{\delta}$ whenever its value is larger than some constant. Thus, we can demonstrate rotational invariance by demonstrating that $\mathbf{x}^\top \boldsymbol{\Sigma}^{-1} \boldsymbol{\delta}$ is rotationally invariant.

$$\begin{aligned}
(\mathbf{W}\mathbf{x})^\top(\mathbf{W}\Sigma\mathbf{W}^\top)^{-1}\mathbf{W}\boldsymbol{\delta} &= \mathbf{x}^\top\mathbf{W}^\top(\mathbf{W}\mathbf{U}\mathbf{S}\mathbf{U}^\top\mathbf{W}^\top)^{-1}\mathbf{W}\boldsymbol{\delta} && \text{by substituting } \mathbf{U}\mathbf{S}\mathbf{U}^\top \text{ for } \Sigma \\
&= \mathbf{x}^\top\mathbf{W}^\top(\tilde{\mathbf{U}}\mathbf{S}\tilde{\mathbf{U}}^\top)^{-1}\mathbf{W}\boldsymbol{\delta} && \text{by letting } \tilde{\mathbf{U}} = \mathbf{W}\mathbf{U} \\
&= \mathbf{x}^\top\mathbf{W}^\top(\tilde{\mathbf{U}}\mathbf{S}^{-1}\tilde{\mathbf{U}}^\top)\mathbf{W}\boldsymbol{\delta} && \text{by the laws of matrix inverse} \\
&= \mathbf{x}^\top\mathbf{W}^\top\mathbf{W}\mathbf{U}\mathbf{S}^{-1}\mathbf{U}^\top\mathbf{W}^\top\mathbf{W}\boldsymbol{\delta} && \text{by un-substituting } \mathbf{W}\mathbf{U} = \tilde{\mathbf{U}} \\
&= \mathbf{x}^\top\mathbf{U}\mathbf{S}^{-1}\mathbf{U}^\top\boldsymbol{\delta} && \text{because } \mathbf{W}^\top\mathbf{W} = \mathbf{I} \\
&= \mathbf{x}^\top\Sigma^{-1}\boldsymbol{\delta} && \text{by un-substituting } \mathbf{U}\mathbf{S}^{-1}\mathbf{U}^\top = \Sigma
\end{aligned}$$

□

One implication of this lemma is that we can reparameterize without loss of generality. Specifically, defining $\mathbf{W} := \mathbf{U}^\top$ yields a change of variables: $\Sigma \mapsto \mathbf{S}$ and $\boldsymbol{\delta} \mapsto \mathbf{U}^\top\boldsymbol{\delta} := \boldsymbol{\delta}''$, where \mathbf{S} is a diagonal covariance matrix. Moreover, let $\mathbf{d} = (\sigma_1, \dots, \sigma_D)^\top$ be the vector of eigenvalues, then $\mathbf{S}^{-1}\boldsymbol{\delta}'' = \mathbf{d}^{-1} \odot \tilde{\boldsymbol{\delta}}$, where \odot is the Hadamard (entrywise) product. The LDA classifier may therefore be encoded by a unit vector, $\tilde{\mathbf{d}} := \frac{1}{m}\mathbf{d}^{-1} \odot \tilde{\boldsymbol{\delta}}$, and its magnitude, $m := \|\mathbf{d}^{-1} \odot \tilde{\boldsymbol{\delta}}\|$. This will be useful later.

B.V Rotation of Projection Based Linear Classifiers

By a similar argument as above, one can easily show that:

$$\begin{aligned}
(\mathbf{A}\mathbf{W}\mathbf{x})^\top(\mathbf{A}\mathbf{W}\Sigma\mathbf{W}^\top\mathbf{A}^\top)^{-1}\mathbf{A}\mathbf{W}\boldsymbol{\delta} &= \mathbf{x}^\top(\mathbf{W}^\top\mathbf{A}^\top)(\mathbf{A}\mathbf{W})\Sigma^{-1}(\mathbf{W}^\top\mathbf{A}^\top)(\mathbf{A}\mathbf{W})\boldsymbol{\delta} \\
&= \mathbf{x}^\top\mathbf{Y}^\top\mathbf{Y}\Sigma^{-1}\mathbf{Y}^\top\mathbf{Y}\boldsymbol{\delta} \\
&= \mathbf{x}^\top\mathbf{Z}\Sigma^{-1}\mathbf{Z}^\top\boldsymbol{\delta} \\
&= \mathbf{x}^\top(\mathbf{Z}\Sigma\mathbf{Z}^\top)^{-1}\boldsymbol{\delta} = \mathbf{x}^\top\tilde{\Sigma}_d^{-1}\boldsymbol{\delta},
\end{aligned}$$

where $\mathbf{Y} = \mathbf{A}\mathbf{W} \in \mathbb{R}^{d \times p}$ so that $\mathbf{Z} = \mathbf{Y}^\top\mathbf{Y}$ is a symmetric $p \times p$ matrix of rank d . In other words, rotating and then projecting is equivalent to a change of basis. The implications of the above is:

Lemma 5. g_A is rotationally invariant if and only if $\text{span}(\mathbf{A}) = \text{span}(\Sigma_d)$. In other words, $r\text{rLDA}$ is the only rotationally invariant projection.

B.VI Low-Rank Canonical Correlation Analysis

We now contrast LOL and low-rank CCA. For discriminant analysis, low-rank CCA corresponds to finding the eigenvectors of $S_X^\dagger S_B$ where

$$S_X = \sum_i (X_i - \bar{X})(X_i - \bar{X})^\top; \quad \bar{X} = \sum_i X_i$$

is the sample covariance matrix of the X_i , S_X^\dagger is the inverse of S_X (or Moore-Penrose pseudo-inverse of S_X if S_X is not invertible), and

$$S_B = \frac{n_0}{n}(\bar{X}_0 - \bar{X})(\bar{X}_0 - \bar{X})^\top + \frac{n_1}{n}(\bar{X}_1 - \bar{X})(\bar{X}_1 - \bar{X})^\top; \quad \bar{X}_j = \sum_{i: Y_i=j} X_i \text{ for } j \in \{0, 1\}$$

is the between class covariance matrix [64]. It is widely known (see section 11.5 of [59]) that if S_X is invertible then the above formulation reduces to that of Fisher L, namely that of finding \hat{v} satisfying

$$\hat{v} = \operatorname{argmax}_{v \neq 0} \frac{v^\top S_B v}{v^\top S_W v}$$

$$S_W = \sum_{i: Y_i=0} (X_i - \bar{X}_0)(X_i - \bar{X}_0)^\top + \sum_{i: Y_i=1} (X_i - \bar{X}_1)(X_i - \bar{X}_1)^\top;$$

where S_W is the pooled within-sample covariance matrix and $S_X = S_W + S_B$. In the context of our current paper where X is assumed to be high-dimensional, it is well-known that S_X is not a good estimator of the population covariance matrix $\Sigma_X = \mathbb{E}[(X - \mu)(X - \mu)^\top]$ and thus computing S_X^{-1} is suboptimal for subsequent inference unless some form of regularization is employed. Our consideration of low-rank linear transformations AX provides one principled approach to regularizations of high-dimensional S_X . In contrast, the above (unregularized) formulation of low-rank CCA frequently yields discrimination direction vectors corresponding to “maximum data piling” (MDP) directions [5, 64] in high-dimensional settings (and always yield maximum data piling directions when $p \geq n$). These MDP directions lead to *perfect* discrimination of the training data, but can suffer from poor generalization performance, as the examples in [5, 64] indicate.

Naïvely computing the low-rank CCA projection requires storing and inverting a $p \times p$ matrix. However, we devised an implementation for low-rank CCA that does not require ever materializing this matrix. Modern eigensolvers compute eigenvalues by performing a sequence of matrix vector multiplication. For example, to compute eigenvalues of S_X , an eigensolver performs $S_X v$ multiple times until the algorithm converges. Assume that the number of iteration is i , the computation complexity of the eigensolver is $O(n \times p \times i)$. Performing pseudo-inverse of S_X computes truncated SVD on S_X , resulting in $S_X v = \sum_i (X_i - \bar{X})(X_i - \bar{X})^\top v$. Here we never physically generate S_X . Instead, we always compute $v' = (X_i - \bar{X})^\top v$ and then $v'' = (X_i - \bar{X})v'$ to compute $S_X v$. Assume k classes, $S_X v$ has the computation complexity of $O(n \times p \times k)$ and the space complexity of $O(n \times p \times k)$. S_X can be decomposed into $U\Sigma V$, where U is a $n \times n$ matrix and V is a $n \times p$ matrix.

$$S_X^\dagger S_B = U\Sigma^{-1}V \left(\frac{n_0}{n} (\bar{X}_0 - \bar{X})(\bar{X}_0 - \bar{X})^\top + \frac{n_1}{n} (\bar{X}_1 - \bar{X})(\bar{X}_1 - \bar{X})^\top \right).$$

Computing eigenvalues of $S_X^\dagger S_B$ requires

$$S_X^\dagger S_B v = U\Sigma^{-1}V \left(\frac{n_0}{n} (\bar{X}_0 - \bar{X})((\bar{X}_0 - \bar{X})^\top v) + \frac{n_1}{n} (\bar{X}_1 - \bar{X})((\bar{X}_1 - \bar{X})^\top v) \right).$$

Similar to $S_X v$, we never physically generate S_X^\dagger or S_B . Instead, we always multiply the terms on the right with v first, which results in the computation complexity of $O(n \times p)$ and the space complexity of $O(n \times p)$. To our knowledge, this algorithm is novel, and the implementation is also of course novel.

C Simulations

Let $f_{x|y}$ denote the conditional distribution of X given Y , and let f_y denote the prior probability of Y . For simplicity, assume that realizations of the random variable X are p -dimensional vectors, $x \in \mathbb{R}^p$, and realizations of the random variable Y are binary, $y \in \{0, 1\}$. For most simulation settings, each class is Gaussian: $f_{x|y} = \mathcal{N}(\mu_y, \Sigma_y)$, where μ_y is the class-conditional mean and Σ_y is the class-conditional covariance. Moreover, we assume f_y is a Bernoulli distribution with probability π that $y = 1$, $f_y = \mathcal{B}(\pi)$. We typically assume that both classes are equally likely, $\pi = 0.5$, and the covariance matrices are the same, $\Sigma_0 = \Sigma_1 = \Sigma$. Under such assumptions, we merely specify $\theta = \{\mu_0, \mu_1, \Sigma\}$. We consider the following simulation settings:

Stacked Cigars

- $\mu_0 = \mathbf{0}$,
- $\mu_1 = (a, b, a, \dots, a)$,
- Σ is a diagonal matrix, with diagonal vector, $\mathbf{d} = (1, b, 1, \dots, 1)$,

where $a = 0.15$ and $b = 4$.

Trunk

- $\mu_0 = b/\sqrt{(1, 3, 5, \dots, 2p)}$,
- $\mu_1 = -\mu_0$,
- Σ is a diagonal matrix, with diagonal vector, $\mathbf{d} = 100/\sqrt{(p, p-1, p-2, \dots, 1)}$,

where $b = 4$.

Rotated Trunk Same as Trunk, but the data are randomly rotated, that is, we sample Q uniformly from the set of p -dimensional rotation matrices, and then set:

- $\mu_0 \leftarrow Q\mu_0$,
- $\mu_1 \leftarrow Q\mu_1$,
- $\Sigma \leftarrow Q\Sigma Q^T$.

3 Classes Same as Trunk, but with a third mean equal to the zero vector, $\mu_2 = \mathbf{0}$.

- $\mu_0 = b/\sqrt{(1, 3, 5, \dots, 2p)}$,
- $\mu_1 = -\mu_0$,
- $\mu_2 = \mathbf{0}$,
- Σ is a diagonal matrix, with diagonal vector, $\mathbf{d} = 100/\sqrt{(p, p-1, p-2, \dots, 1)}$,

where $b = 4$.

Robust An experiment in which outliers are present for estimation of the projection matrix, but removed for training and testing of the classifier. This is due to the strong amount of noise present in the robust experiment will lead to poor generalizability of the estimated LDA classifier. Parameters indexed by i correspond to the generative model for the inliers, and those with o correspond to the outliers.

- $\mu_0^{(i)} = b/\sqrt{(1, 3, 5, \dots, p)}$ for the first $p/2$ dimensions and 0 otherwise,
- $\mu_1^{(i)} = -\mu_0$,
- $\Sigma^{(i)} = b^3/\sqrt{(1, 2, \dots, p)}$,
- $\mu^{(o)} = \mathbf{0}$,
- $\Sigma^{(o)} = b^6/\sqrt{(1, 2, \dots, p)}$,
- $\pi^{(i)} = 0.7$,
- $\pi^{(o)} = 0.3$,

and outliers are randomly assigned class 0 or class 1 with equal probability.

Cross An experiment in which the two classes have identical means but different covariance matrices, meaning the optimal discriminant boundary is quadratic.

- $\mu_0 = \mu_1 = \mathbf{0}$,

- Σ_0 is a diagonal matrix, with diagonal $(a, \dots, a, b, \dots, b)$ where the first $\frac{d}{3}$ elements are a , and the rest are b ,
- Σ_1 is a diagonal matrix, with diagonal $(b, \dots, b, a, \dots, a, b, \dots, b)$ where the middle $\frac{d}{3}$ elements are a , and the others are b ,

and we let $a = 1$, and $b = \frac{1}{4}$.

Hump- K An experiment with K classes, in which the class means display an alternating series of humps, and the class covariance is a scalar multiple of the identity.

- $\pi_k = \frac{1}{K}$
- $x_{l,k} = \lfloor -\frac{K}{2} \rfloor$ the left endpoint of the hump
- $x_{r,k} = d - x_{l,K-k+1}$ the right endpoint of the hump
- $x_{m,k} = \lfloor \frac{x_{l,k} + x_{r,k}}{2} \rfloor$ the midpoint of the hump
- Let a_k, b_k, c_k be the unique coefficients such that $c_k + b_k x + a_k x^2$ passes through $x_{l,k}$ at $y = 0$, passes through $x_{r,k}$ at $y = b$, and passes through $x_{m,k}$ at $y = 0$.
- Let $\alpha_k = \begin{cases} 1 & k \text{ is odd} \\ -1 & k \text{ is even} \end{cases}$
- for $j = 1, \dots, d$, let $\mu_{k,j} = \begin{cases} 0 & j \notin [x_{l,k}, x_{r,k}] \\ c_k + b_k j + a_k j^2 & j \in [x_{l,k}, x_{r,k}] \end{cases}$
- Σ is a diagonal matrix, with diagonal vector (σ, \dots, σ) .

where $b = 4$ and $\sigma = \frac{100}{K}$.

Computational Efficiency Experiments These experiments used the Trunk setting, increasing the observed dimensionality.

Hypothesis Testing Experiments We considered two related joint distributions here. The first joint (Diagonal) is described by:

- $\mu_0 = \mathbf{0}$,
- $\tilde{\mu}_1 \sim \mathcal{N}(\mathbf{0}, \mathbf{I})$, $\mu_1 = \tilde{\mu}_1 / \|\tilde{\mu}_1\|$,
- Σ is the same Toeplitz matrix (where the top row is $\rho^{(0,1,2,\dots,p-1)}$), and the matrix is rescaled to have a Frobenius norm of 50.

The second (Dense) is the same except that the eigenvectors are uniformly random sampled orthonormal matrices, rather than the identity matrix.

Regression Experiments In this experiment we used a distribution similar to the Toeplitz distribution as described above, but y was a linear function of x , that is, $y = Ax$, where $x \sim \mathcal{N}(\mathbf{0}, \Sigma)$, where Σ is the above described Toeplitz matrix, and A is a diagonal matrix whose first two diagonal elements are non-zero, and the rest are zero.

D Theorems and Proofs of Main Result

D.1 Chernoff information

We now introduce the notion of the Chernoff information, which serves as our surrogate measure for the Bayes error of any classification procedure given the *projected* data. Our discussion of the Chernoff information is under the context of decision rules for hypothesis testing, nevertheless, as evidenced by the fact that the *maximum a posteriori* decision rule—equivalently the Bayes classifier—achieves the Chernoff information rate, this distinction between hypothesis testing and classification is mainly for ease of exposition.

Let F_0 and F_1 be two absolutely continuous multivariate distributions in $\Omega \subset \mathbb{R}^d$ with density functions f_0 and f_1 , respectively. Suppose that X_1, X_2, \dots, X_m are independent and identically distributed random variables, with X_i distributed either F_0 or F_1 . We are interested in testing the simple null hypothesis $\mathbb{H}_0: F = F_0$ against the simple alternative hypothesis $\mathbb{H}_1: F = F_1$. A test T is a sequence of mapping $T_m: \Omega^m \mapsto \{0, 1\}$ such that given $X_1 = x_1, X_2 = x_2, \dots, X_m = x_m$, the test rejects \mathbb{H}_0 in favor of \mathbb{H}_1 if $T_m(x_1, x_2, \dots, x_m) = 1$; similarly, the test decides \mathbb{H}_1 instead of \mathbb{H}_0 if $T_m(x_1, x_2, \dots, x_m) = 0$. The Neyman-Pearson lemma states that, given $X_1 = x_1, X_2 = x_2, \dots, X_m = x_m$ and a threshold $\eta_m \in \mathbb{R}$, the likelihood ratio test rejects \mathbb{H}_0 in favor of \mathbb{H}_1 whenever

$$\left(\sum_{i=1}^m \log f_0(x_i) - \sum_{i=1}^m \log f_1(x_i) \right) \leq \eta_m.$$

Moreover, the likelihood ratio test is the most powerful test at significance level $\alpha_m = \alpha(\eta_m)$, i.e., the likelihood ratio test minimizes the type II error β_m subject to the constraint that the type I error is at most α_m .

Assume that $\pi \in (0, 1)$ is a prior probability of \mathbb{H}_0 being true. Then, for a given $\alpha_m^* \in (0, 1)$, let $\beta_m^* = \beta_m^*(\alpha_m^*)$ be the type II error associated with the likelihood ratio test when the type I error is at most α_m^* . The quantity $\inf_{\alpha_m^* \in (0, 1)} \pi \alpha_m^* + (1 - \pi) \beta_m^*$ is then the Bayes risk in deciding between \mathbb{H}_0 and \mathbb{H}_1 given the m independent random variables X_1, X_2, \dots, X_m . A classical result of Chernoff [23] states that the Bayes risk is intrinsically linked to a quantity known as the *Chernoff information*. More specifically, let $C(F_0, F_1)$ be the quantity

$$\begin{aligned} C(F_0, F_1) &= -\log \left[\inf_{t \in (0, 1)} \int_{\mathbb{R}^d} f_0^t(\mathbf{x}) f_1^{1-t}(\mathbf{x}) d\mathbf{x} \right] \\ &= \sup_{t \in (0, 1)} \left[-\log \int_{\mathbb{R}^d} f_0^t(\mathbf{x}) f_1^{1-t}(\mathbf{x}) d\mathbf{x} \right] \end{aligned} \quad (9)$$

Then we have

$$\lim_{m \rightarrow \infty} \frac{1}{m} \inf_{\alpha_m^* \in (0, 1)} \log(\pi \alpha_m^* + (1 - \pi) \beta_m^*) = -C(F_0, F_1). \quad (10)$$

Thus $C(F_0, F_1)$ is the *exponential* rate at which the Bayes error $\inf_{\alpha_m^* \in (0, 1)} \pi \alpha_m^* + (1 - \pi) \beta_m^*$ decreases as $m \rightarrow \infty$; we also note that the $C(F_0, F_1)$ is independent of π . We also define, for a given $t \in (0, 1)$ the Chernoff divergence $C_t(F_0, F_1)$ between F_0 and F_1 by

$$C_t(F_0, F_1) = -\log \int_{\mathbb{R}^d} f_0^t(\mathbf{x}) f_1^{1-t}(\mathbf{x}) d\mathbf{x}.$$

The Chernoff divergence is an example of a f -divergence as defined in [28]. When $t = 1/2$, $C_t(F_0, F_1)$ is the Bhattacharyya distance between F_0 and F_1 .

The result of Eq. (10) can be extended to $K + 1 \geq 2$ hypothesis, with the exponential rate being the minimum of the Chernoff information between any pair of hypothesis. More specifically, let F_0, F_1, \dots, F_K be distributions on \mathbb{R}^d and let X_1, X_2, \dots, X_m be independent and identically distributed random variables with distribution $F \in \{F_0, F_1, \dots, F_K\}$. Our inference task is in determining the distribution of the X_i among the $K + 1$ hypothesis $\mathbb{H}_0: F = F_0, \dots, \mathbb{H}_K: F = F_K$. Suppose also that hypothesis \mathbb{H}_k has *a priori* probability π_k . For any decision rule g , the risk of g is $r(g) = \sum_k \pi_k \sum_{l \neq k} \alpha_{lk}(g)$ where $\alpha_{lk}(g)$ is the probability of accepting hypothesis \mathbb{H}_l when hypothesis \mathbb{H}_k is true. Then we have [52]

$$\inf_g \lim_{m \rightarrow \infty} \frac{r(g)}{m} = -\min_{k \neq l} C(F_k, F_l), \quad (11)$$

where the infimum is over all decision rules g , i.e., for any g , $r(g)$ decreases to 0 as $m \rightarrow \infty$ at a rate no faster than $\exp(-m \min_{k \neq l} C(F_k, F_l))$.

When the distributions F_0 and F_1 are multivariate normal, that is, $F_0 = \mathcal{N}(\mu_0, \Sigma_0)$ and $F_1 = \mathcal{N}(\mu_1, \Sigma_1)$; then, denoting by $\Sigma_t = t\Sigma_0 + (1 - t)\Sigma_1$, we have

$$C(F_0, F_1) = \sup_{t \in (0,1)} \left(\frac{t(1-t)}{2} (\mu_1 - \mu_0)^\top \Sigma_t^{-1} (\mu_1 - \mu_0) + \frac{1}{2} \log \frac{|\Sigma_t|}{|\Sigma_0|^t |\Sigma_1|^{1-t}} \right).$$

D.II Projecting data and Chernoff information

We now discuss how the Chernoff information characterizes the effect a linear transformation A of the data has on classification accuracy. We start with the following simple result whose proof follows directly from Eq. (11).

Lemma 6. *Let $F_0 = \mathcal{N}(\mu_0, \Sigma)$ and $F_1 \sim \mathcal{N}(\mu_1, \Sigma)$ be two multivariate normals with equal covariance matrices. For any linear transformation A , let $F_0^{(A)}$ and $F_1^{(A)}$ denote the distribution of AX when $X \sim F_0$ and $X \sim F_1$, respectively. We then have*

$$\begin{aligned} C(F_0^{(A)}, F_1^{(A)}) &= \frac{1}{8} (\mu_1 - \mu_0)^\top A^\top (A \Sigma A^\top)^{-1} A (\mu_1 - \mu_0) \\ &= \frac{1}{8} (\mu_1 - \mu_0)^\top \Sigma^{-1/2} \Sigma^{1/2} A^\top (A \Sigma A^\top)^{-1} A \Sigma^{1/2} \Sigma^{-1/2} (\mu_1 - \mu_0) \\ &= \frac{1}{8} \|P_{\Sigma^{1/2} A^\top} \Sigma^{-1/2} (\mu_1 - \mu_0)\|_F^2 \end{aligned} \quad (12)$$

where $P_Z = Z(Z^\top Z)^{-1} Z^\top$ denotes the matrix corresponding to the orthogonal projection onto the columns of Z .

Thus for a classification problem where $X|Y = 0$ and $X|Y = 1$ are distributed multivariate normals with mean μ_0 and μ_1 and the same covariance matrix Σ , Lemma 6 then states that for any two linear transformations A and B , the transformed data AX is to be preferred over the transformed data BX if

$$(\mu_1 - \mu_0)^\top A^\top (A \Sigma A^\top)^{-1} A (\mu_1 - \mu_0) > (\mu_1 - \mu_0)^\top B^\top (B \Sigma B^\top)^{-1} B (\mu_1 - \mu_0).$$

In particular, using Lemma 6, we obtain the following result showing the dominance of `LOL` over reduced-rank `LDA` (or simply `rrLDA` for brevity) when the class conditional distributions are multivariate normal with a common variance.

Theorem 1. Let $F_0 = N(\mu_0, \Sigma)$ and $F_1 \sim N(\mu_1, \Sigma)$ be multivariate normal distributions in \mathbb{R}^p . Let $\lambda_1 \geq \lambda_2 \geq \dots \geq \lambda_p$ be the eigenvalues of Σ and u_1, u_2, \dots, u_p the corresponding eigenvectors. For $d \leq p$, let $U_d = [u_1 \mid u_2 \mid \dots \mid u_d] \in \mathbb{R}^{p \times d}$ be the matrix whose columns are the eigenvectors u_1, u_2, \dots, u_d . Let $A = [\delta \mid U_{d-1}]$ and $B = U_d$ be the LOL and rLDA linear transformations into \mathbb{R}^d , respectively. Then

$$\begin{aligned} C(F_0^{(A)}, F_1^{(A)}) - C(F_0^{(B)}, F_1^{(B)}) &= \frac{(\delta^\top (I - U_{d-1} U_{d-1}^\top) \delta)^2}{\delta^\top (\Sigma - \Sigma_{d-1}) \delta} - \delta^\top (\Sigma_d^\dagger - \Sigma_{d-1}^\dagger) \delta \\ &\geq \frac{1}{\lambda_d} \delta^\top (I - U_{d-1} U_{d-1}^\top) \delta - \frac{1}{\lambda_d} \delta^\top (U_d U_d^\top - U_{d-1} U_{d-1}^\top) \delta \geq 0 \end{aligned} \quad (13)$$

and the inequality is strict whenever $\delta^\top (I - U_d U_d^\top) \delta > 0$.

Proof. We first note that

$$A \Sigma A^\top = [\delta \mid U_{d-1}]^\top \Sigma [\delta \mid U_{d-1}] = \begin{bmatrix} \delta^\top \Sigma \delta & \delta^\top \Sigma U_{d-1} \\ U_{d-1}^\top \Sigma \delta & U_{d-1}^\top \Sigma U_{d-1} \end{bmatrix} = \begin{bmatrix} \delta^\top \Sigma \delta & \delta^\top \Sigma U_{d-1} \\ U_{d-1}^\top \Sigma \delta & \Lambda_{d-1} \end{bmatrix}$$

where $\Lambda_{d-1} = \text{diag}(\lambda_1, \lambda_2, \dots, \lambda_{d-1})$ is the $(d-1) \times (d-1)$ diagonal matrix formed by the eigenvalues $\lambda_1, \lambda_2, \dots, \lambda_{d-1}$. Therefore, letting $\gamma = \delta^\top \Sigma \delta - \delta^\top \Sigma U_{d-1} \Lambda_{d-1}^{-1} U_{d-1}^\top \Sigma \delta$, we have

$$\begin{aligned} (A \Sigma A^\top)^{-1} &= \begin{bmatrix} \delta^\top \Sigma \delta & \delta^\top \Sigma U_{d-1} \\ U_{d-1}^\top \Sigma \delta & U_{d-1}^\top \Sigma U_{d-1} \end{bmatrix}^{-1} \\ &= \begin{bmatrix} \gamma^{-1} & -\delta^\top \Sigma U_{d-1} \Lambda_{d-1}^{-1} \gamma^{-1} \\ -\Lambda_{d-1}^{-1} U_{d-1}^\top \Sigma \delta \gamma^{-1} & (\Lambda_{d-1} - \frac{U_{d-1}^\top \Sigma \delta \delta^\top \Sigma U_{d-1}}{\delta^\top \Sigma \delta})^{-1} \end{bmatrix}. \end{aligned}$$

The Sherman-Morrison-Woodbury formula then implies

$$\begin{aligned} \left(\Lambda_{d-1} - \frac{U_{d-1}^\top \Sigma \delta \delta^\top \Sigma U_{d-1}}{\delta^\top \Sigma \delta} \right)^{-1} &= \Lambda_{d-1}^{-1} + \frac{\Lambda_{d-1}^{-1} U_{d-1}^\top \Sigma \delta \delta^\top \Sigma U_{d-1} \Lambda_{d-1}^{-1} / (\delta^\top \Sigma \delta)}{1 - \delta^\top \Sigma U_{d-1} \Lambda_{d-1}^{-1} U_{d-1}^\top \Sigma \delta / (\delta^\top \Sigma \delta)} \\ &= \Lambda_{d-1}^{-1} + \frac{\Lambda_{d-1}^{-1} U_{d-1}^\top \Sigma \delta \delta^\top \Sigma U_{d-1} \Lambda_{d-1}^{-1}}{\delta^\top \Sigma \delta - \delta^\top \Sigma U_{d-1} \Lambda_{d-1}^{-1} U_{d-1}^\top \Sigma \delta} \\ &= \Lambda_{d-1}^{-1} + \gamma^{-1} \Lambda_{d-1}^{-1} U_{d-1}^\top \Sigma \delta \delta^\top \Sigma U_{d-1} \Lambda_{d-1}^{-1} \end{aligned}$$

We note that $\Sigma U_{d-1} = U_{d-1} \Lambda_{d-1}$ and $U_{d-1}^\top \Sigma = \Lambda_{d-1} U_{d-1}^\top$ and hence

$$\begin{aligned} \gamma &= \delta^\top \Sigma \delta - \delta^\top \Sigma U_{d-1} \Lambda_{d-1}^{-1} U_{d-1}^\top \Sigma \delta = \delta^\top \Sigma \delta - \delta^\top U_{d-1} \Lambda_{d-1} \Lambda_{d-1}^{-1} \Lambda_{d-1} U_{d-1}^\top \delta \\ &= \delta^\top \Sigma \delta - \delta^\top U_{d-1} \Lambda_{d-1} U_{d-1}^\top \delta = \delta^\top (\Sigma - \Sigma_{d-1}) \delta \end{aligned}$$

where $\Sigma_{d-1} = U_{d-1} \Lambda_{d-1} U_{d-1}^\top$ is the best rank $d-1$ approximation to Σ with respect to any unitarily invariant norm. In addition,

$$\Lambda_{d-1}^{-1} U_{d-1}^\top \Sigma \delta \delta^\top \Sigma U_{d-1} \Lambda_{d-1}^{-1} = \Lambda_{d-1}^{-1} \Lambda_{d-1} U_{d-1}^\top \delta \delta^\top U_{d-1} \Lambda_{d-1} \Lambda_{d-1}^{-1} = U_{d-1}^\top \delta \delta^\top U_{d-1}.$$

We thus have

$$(A \Sigma A^\top)^{-1} = \begin{bmatrix} \gamma^{-1} & -\delta^\top \Sigma U_{d-1} \Lambda_{d-1}^{-1} \gamma^{-1} \\ -\Lambda_{d-1}^{-1} U_{d-1}^\top \Sigma \delta \gamma^{-1} & (\Lambda_{d-1} - \frac{U_{d-1}^\top \Sigma \delta \delta^\top \Sigma U_{d-1}}{\delta^\top \Sigma \delta})^{-1} \end{bmatrix} = \begin{bmatrix} \gamma^{-1} & -\gamma^{-1} \delta^\top U_{d-1} \\ -\gamma^{-1} U_{d-1}^\top \delta & \Lambda_{d-1}^{-1} + \gamma^{-1} U_{d-1}^\top \delta \delta^\top U_{d-1} \end{bmatrix}.$$

Therefore,

$$\begin{aligned}
\delta^\top A^\top (A \Sigma A^\top)^{-1} A \delta &= \delta^\top [\delta \mid U_{d-1}] \begin{bmatrix} \gamma^{-1} & -\gamma^{-1} \delta^\top U_{d-1} \\ -\gamma^{-1} U_{d-1}^\top \delta & \Lambda_{d-1}^{-1} + \gamma^{-1} U_{d-1}^\top \delta \delta^\top U_{d-1} \end{bmatrix} [\delta \mid U_{d-1}]^\top \delta \\
&= [\delta^\top \delta \mid \delta^\top U_{d-1}] \begin{bmatrix} \gamma^{-1} & -\gamma^{-1} \delta^\top U_{d-1} \\ -\gamma^{-1} U_{d-1}^\top \delta & \Lambda_{d-1}^{-1} + \gamma^{-1} U_{d-1}^\top \delta \delta^\top U_{d-1} \end{bmatrix} \begin{bmatrix} \delta^\top \delta \\ U_{d-1}^\top \delta \end{bmatrix} \\
&= \gamma^{-1} (\delta^\top \delta)^2 - 2\gamma^{-1} \delta^\top \delta \delta^\top U_{d-1} U_{d-1}^\top \delta + \delta^\top U_{d-1} (\Lambda_{d-1}^{-1} + \gamma^{-1} U_{d-1}^\top \delta \delta^\top U_{d-1}) U_{d-1}^\top \delta \\
&= \gamma^{-1} (\delta^\top \delta - \delta^\top U_{d-1} U_{d-1}^\top \delta)^2 + \delta^\top U_{d-1} \Lambda_{d-1}^{-1} U_{d-1}^\top \delta \\
&= \gamma^{-1} (\delta^\top (I - U_{d-1} U_{d-1}^\top) \delta)^2 + \delta^\top \Sigma_{d-1}^\dagger \delta
\end{aligned}$$

where Σ_{d-1}^\dagger is the Moore-Penrose pseudo-inverse of Σ_{d-1} . The LDA projection matrix into \mathbb{R}^d is given by $B = U_d^\top$ and hence

$$\delta^\top B^\top (B \Sigma B^\top)^{-1} B \delta = \delta^\top U_d \Lambda_d^{-1} U_d^\top \delta = \delta^\top \Sigma_d^\dagger \delta. \quad (14)$$

We thus have

$$\begin{aligned}
C(F_0^{(A)}, F_1^{(A)}) - C(F_0^{(B)}, F_1^{(B)}) &= \gamma^{-1} (\delta^\top (I - U_{d-1} U_{d-1}^\top) \delta)^2 - \delta^\top (\Sigma_d^\dagger - \Sigma_{d-1}^\dagger) \delta \\
&= \frac{(\delta^\top (I - U_{d-1} U_{d-1}^\top) \delta)^2}{\delta^\top (\Sigma - \Sigma_{d-1}) \delta} - \delta^\top (\Sigma_d^\dagger - \Sigma_{d-1}^\dagger) \delta \\
&\geq \frac{(\delta^\top (I - U_{d-1} U_{d-1}^\top) \delta)^2}{\lambda_d \delta^\top (I - U_{d-1} U_{d-1}^\top) \delta} - \frac{1}{\lambda_d} \delta^\top u_d u_d^\top \delta \\
&= \frac{1}{\lambda_d} \delta^\top (I - U_{d-1} U_{d-1}^\top) \delta - \frac{1}{\lambda_d} \delta^\top (U_d U_d^\top - U_{d-1} U_{d-1}^\top) \delta \geq 0
\end{aligned}$$

where we recall that u_d is the d -th column of U_d . Thus $C(F_0^{(A)}, F_1^{(A)}) \geq C(F_0^{(B)}, F_1^{(B)})$ always, and the inequality is strict whenever $\delta^\top (I - U_d U_d^\top) \delta > 0$. \square

Remark 1. *Theorem 1 can be extended to the case wherein the linear transformations are $A = [\delta \mid U_{d-1}]$ and $B = U_d$, respectively, such that U_d is an arbitrary $p \times d$ matrix with $U_d^\top U_d = I$, and U_{d-1} is the first $d-1$ columns of U_d . A similar derivation to that in the proof of Theorem 1 then yields*

$$C(F_0^{(A)}, F_1^{(A)}) = \frac{(\delta^\top \Sigma^{-1/2} (I - V_{d-1} V_{d-1}^\top) \Sigma^{1/2} \delta)^2}{\delta^\top \Sigma^{1/2} (I - V_{d-1} V_{d-1}^\top) \Sigma^{1/2} \delta} + \delta^\top \Sigma^{-1/2} V_{d-1} V_{d-1}^\top \Sigma^{-1/2} \delta \quad (15)$$

$$C(F_0^{(B)}, F_1^{(B)}) = \delta^\top \Sigma^{-1/2} V_d V_d^\top \Sigma^{-1/2} \delta \quad (16)$$

where $V_d V_{d-1}^\top = \Sigma^{1/2} U_d (U_d^\top \Sigma U_d)^{-1} U_d^\top \Sigma^{1/2}$ is the orthogonal projection onto the column space of $\Sigma^{1/2} U_d$. Hence $C(F_0^{(A)}, F_1^{(A)}) > C(F_0^{(B)}, F_1^{(B)})$ if and only if

$$\frac{(\delta^\top \Sigma^{-1/2} (I - V_{d-1} V_{d-1}^\top) \Sigma^{1/2} \delta)^2}{\delta^\top \Sigma^{1/2} (I - V_{d-1} V_{d-1}^\top) \Sigma^{1/2} \delta} > \delta^\top \Sigma^{-1/2} (V_d V_d^\top - V_{d-1} V_{d-1}^\top) \Sigma^{-1/2} \delta. \quad (17)$$

We recover Eq. 13 by letting U_d be the matrix whose columns are the eigenvectors corresponding to the d largest eigenvalue of Σ .

We next present a result relating the Chernoff information for LOL and rrLDA.

Theorem 2. Assume the setting of Theorem 1. Let $C = \tilde{U}_d^\top$ where \tilde{U}_d is the $p \times d$ matrix whose columns are the d largest eigenvectors of the pooled covariance matrix $\tilde{\Sigma} = \mathbb{E}[(X - \frac{\mu_0 + \mu_1}{2})(X - \frac{\mu_0 + \mu_1}{2})^\top]$. Then C is the linear transformation for PCA and

$$\begin{aligned} C(F_0^{(A)}, F_1^{(A)}) - C(F_0^{(C)}, F_1^{(C)}) &= \frac{(\delta^\top(I - U_{d-1}U_{d-1}^\top)\delta)^2}{\delta^\top(\Sigma - \Sigma_{d-1})\delta} + \delta^\top \Sigma_{d-1}^\dagger \delta - \delta^\top \tilde{\Sigma}_d^\dagger \delta - \frac{(\delta^\top \tilde{\Sigma}_d^\dagger \delta)^2}{4 - \delta^\top \tilde{\Sigma}_d^\dagger \delta} \\ &= \frac{(\delta^\top(I - U_{d-1}U_{d-1}^\top)\delta)^2}{\delta^\top(\Sigma - \Sigma_{d-1})\delta} + \delta^\top \Sigma_{d-1}^\dagger \delta - \frac{4\delta^\top \tilde{\Sigma}_d^\dagger \delta}{4 - \delta^\top \tilde{\Sigma}_d^\dagger \delta}. \end{aligned} \quad (18)$$

where $\tilde{\Sigma}_d = \tilde{U}_d \tilde{S}_d \tilde{U}_d^\top$ is the best rank d approximation to $\tilde{\Sigma} = \Sigma + \frac{1}{4}\delta\delta^\top$.

Proof. Assume, without loss of generality, that $\mu_1 = -\mu_0 = \mu$. We then have

$$\tilde{\Sigma} = \mathbb{E}[XX^\top] = \pi\Sigma + \pi\mu_0\mu_0^\top + (1-\pi)\Sigma + (1-\pi)\mu_1\mu_1^\top = \Sigma + \mu\mu^\top = \Sigma + \frac{1}{4}\delta\delta^\top.$$

Therefore

$$(C\Sigma C^\top)^{-1} = (\tilde{U}_d^\top \Sigma \tilde{U}_d)^{-1} = (\tilde{U}_d^\top (\tilde{\Sigma} - \frac{1}{4}\delta\delta^\top) \tilde{U}_d)^{-1} = (\tilde{S}_d - \frac{1}{4}\tilde{U}_d^\top \delta\delta^\top \tilde{U}_d)^{-1} = \tilde{S}_d^{-1} + \frac{\tilde{S}_d^{-1} \tilde{U}_d^\top \delta\delta^\top \tilde{U}_d \tilde{S}_d^{-1}}{4 - \delta^\top \tilde{U}_d \tilde{S}_d^{-1} \tilde{U}_d^\top \delta}$$

where \tilde{S}_d is the diagonal matrix containing the d largest eigenvalues of $\tilde{\Sigma}$. Hence

$$\begin{aligned} C(F_0^{(C)}, F_1^{(C)}) &= \delta^\top C^\top (C\Sigma C^\top)^{-1} C \delta = \delta^\top \tilde{U}_d \left(\tilde{S}_d^{-1} + \frac{\tilde{S}_d^{-1} \tilde{U}_d^\top \delta\delta^\top \tilde{U}_d \tilde{S}_d^{-1}}{4 - \delta^\top \tilde{U}_d \tilde{S}_d^{-1} \tilde{U}_d^\top \delta} \right) \tilde{U}_d^\top \delta \\ &= \delta^\top \tilde{U}_d \tilde{S}_d^{-1} \tilde{U}_d^\top \delta + \frac{(\delta^\top \tilde{U}_d \tilde{S}_d^{-1} \tilde{U}_d^\top \delta)^2}{4 - \delta^\top \tilde{U}_d \tilde{S}_d^{-1} \tilde{U}_d^\top \delta} \\ &= \delta^\top \tilde{\Sigma}_d^\dagger \delta + \frac{(\delta^\top \tilde{\Sigma}_d^\dagger \delta)^2}{4 - \delta^\top \tilde{\Sigma}_d^\dagger \delta} = \frac{4\delta^\top \tilde{\Sigma}_d^\dagger \delta}{4 - \delta^\top \tilde{\Sigma}_d^\dagger \delta}. \end{aligned} \quad (19)$$

as desired. \square

Remark 2. We recall that the LOL projection $A = [\delta \mid U_{d-1}]^\top$ yields

$$C(F_0^{(A)}, F_1^{(A)}) = \frac{(\delta^\top(I - U_{d-1}U_{d-1}^\top)\delta)^2}{\delta^\top(\Sigma - \Sigma_{d-1})\delta} + \delta^\top \Sigma_{d-1}^\dagger \delta.$$

To illustrate the difference between the LOL projection and that based on the eigenvectors of the pooled covariance matrix, consider the following simple example. Let $\Sigma = \text{diag}(\lambda_1, \lambda_2, \dots, \lambda_p)$ be a diagonal matrix with $\lambda_1 \geq \lambda_2 \geq \dots \geq \lambda_p$. Also let $\delta = (0, 0, \dots, 0, s)$. Suppose furthermore that $\lambda_p + s^2/4 < \lambda_d$. Then we have $\tilde{\Sigma}_d = \text{diag}(\lambda_1, \lambda_2, \dots, \lambda_d, 0, 0, \dots, 0)$. Thus $\tilde{\Sigma}_d^\dagger = \text{diag}(1/\lambda_1, 1/\lambda_2, \dots, 1/\lambda_d, 0, 0, \dots, 0)$ and $\delta^\top \tilde{\Sigma}_d^\dagger \delta = 0$. Therefore, $C(F_0^{(B)}, F_1^{(B)}) = 0$.

On the other hand, we have

$$C(F_0^{(A)}, F_1^{(A)}) = \frac{(\delta^\top(I - U_{d-1}U_{d-1}^\top)\delta)^2}{\delta^\top(\Sigma - \Sigma_{d-1})\delta} + \delta^\top \Sigma_{d-1}^\dagger \delta = \frac{s^4}{s^2\lambda_p} + 0 = s^2/\lambda_p.$$

A more general form of the previous observation is the following result which shows that LOL is preferable over PCA when the dimension p is sufficiently large.

Proposition 1. Let Σ be a $p \times p$ covariance matrix of the form

$$\Sigma = \begin{bmatrix} \Sigma_d & 0 \\ 0 & \Sigma_d^\perp \end{bmatrix}$$

where Σ_d is a $d \times d$ matrix. Let $\lambda_1 \geq \lambda_2 \geq \dots \geq \lambda_p$ be the eigenvalues of Σ , with $\lambda_1, \lambda_2, \dots, \lambda_d$ being the eigenvalues of Σ_d . Suppose that the entries of δ are i.i.d. with the following properties.

1. $\delta_i \sim Y_i * N(\tau, \sigma^2)$ where $Y_1, Y_2, \dots, Y_p \stackrel{\text{i.i.d.}}{\sim} \text{Bernoulli}(1 - \epsilon)$.
2. $p(1 - \epsilon) \rightarrow \theta$ as $p \rightarrow \infty$ for some constant θ .

Then there exists a constant $C > 0$ such that if $\lambda_d - \lambda_{d+1} \geq C\theta\tau^2 \log p$, then, with probability at least ϵ^d

$$C(F_0^{(A)}, F_1^{(A)}) > C(F_0^{(B)}, F_1^{(B)}) = 0$$

Proof. The above construction of Σ and δ implies, with probability at least ϵ^d , that the covariance matrix for $\tilde{\Sigma}$ is of the form

$$\tilde{\Sigma} = \begin{bmatrix} \Sigma_d & 0 \\ 0 & \Sigma_d^\perp + \frac{1}{4}(\tilde{\delta}\tilde{\delta}^\top) \end{bmatrix}$$

where $\tilde{\delta} \in \mathbb{R}^{p-d}$ is formed by excluding the first d elements of δ . Now, if $\lambda_{d+1} + \frac{1}{4}\|\tilde{\delta}\|^2 < \lambda_d$, then the d largest eigenvalues of $\tilde{\Sigma}$ are still $\lambda_1, \lambda_2, \dots, \lambda_d$, and thus the eigenvectors corresponding to the d largest eigenvalues of $\tilde{\Sigma}$ are the same as those for the d largest eigenvalues of Σ . That is to say,

$$\lambda_{d+1} + \frac{1}{4}\|\tilde{\delta}\|^2 < \lambda_d \implies \tilde{\Sigma}_d^\dagger = \Sigma_d^\dagger \implies \delta^\top \tilde{\Sigma}_d^\dagger \delta = 0 \implies C(F_0^{(B)}, F_1^{(B)}) = 0.$$

We now compute the probability that $\lambda_{d+1} + \frac{1}{4}\|\tilde{\delta}\|^2 < \lambda_d$. Suppose for now that $\epsilon > 0$ is fixed and does not vary with p . We then have

$$\frac{\sum_{i=d+1}^p \delta_i^2 - (p-d)(1-\epsilon)\tau^2}{\sqrt{(p-d)(2(1-\epsilon)(2\tau^2\sigma^2 + \sigma^4) + \epsilon(1-\epsilon)(\tau^4 + 2\tau^2\sigma^2 + \sigma^4))}} \xrightarrow{d} N(0, 1).$$

Thus, as $p \rightarrow \infty$, the probability that $\lambda_{d+1} + \frac{1}{4}\|\tilde{\delta}\|^2 < \lambda_d$ converges to that of

$$\Phi\left(\frac{4(\lambda_d - \lambda_{d+1}) - (p-d)(1-\epsilon)\tau^2}{\sqrt{(p-d)(2(1-\epsilon)(2\tau^2\sigma^2 + \sigma^4) + \epsilon(1-\epsilon)(\tau^4 + 2\tau^2\sigma^2 + \sigma^4))}}\right).$$

This probability can be made arbitrarily close to 1 provided that $\lambda_d - \lambda_{d+1} \geq Cp(1-\epsilon)\tau^2$ for all sufficiently large p and for some constant $C > 1/4$. Since the probability that $\delta_1 = \delta_2 = \dots = \delta_d$ is at least ϵ^d , we thus conclude that for sufficiently large p , with probability at least ϵ^d ,

$$C(F_0^{(B)}, F_1^{(B)}) = 0 < C(F_0^{(A)}, F_1^{(A)}).$$

In the case where $\epsilon = \epsilon(p) \rightarrow 1$ as $p \rightarrow \infty$ such that $p(1-\epsilon) \rightarrow \theta$ for some constant θ , then the probability that $\lambda_{d+1} + \frac{1}{4}\|\tilde{\delta}\|^2 < \lambda_d$ converges to the probability that

$$\frac{1}{4} \sum_{i=1}^K \sigma^2 \chi_1^2(\tau) \geq \lambda_d - \lambda_{d+1}$$

where K is Poisson distributed with mean θ and $\chi_1^2(\tau)$ is the non-central chi-square distribution with one degree of freedom and non-centrality parameter τ . Thus if $\lambda_d - \lambda_{d+1} \geq C\theta\tau^2 \log p$ for sufficiently large p and for some constant C , then this probability can also be made arbitrarily close to 1. \square

Remark 3. *The previous comparisons are done for the case of $C = 2$ classes. Extending these comparisons to the case of $C > 2$ classes is, however, non-trivial. More precisely, suppose we have $Y \in \{1, 2, \dots, C\}$ and that, conditional on $Y = c$, $X \sim \mathcal{N}(\mu_c, \Sigma)$ is multivariate normal with mean μ_c and common covariance matrix Σ . Then, given $X = x$, the Bayes optimal classifier for Y is still*

$$g_{\text{LDA}}(x) = \operatorname{argmin}_{y \in \{1, 2, \dots, C\}} \left[\frac{1}{2}(x - \mu_y)^\top \Sigma^{-1}(x - \mu_y) - \log \pi_y \right] = \operatorname{argmin}_{y \in \{1, 2, \dots, C\}} \left[-x^\top \Sigma^{-1} \mu_y + \frac{1}{2} \mu_y^\top \Sigma^{-1} \mu_y - \log \pi_y \right]$$

Taking $\frac{1}{2} \mu_y^\top \Sigma^{-1} \mu_y - \log \pi_y$ as either a given constant or as an intercept term to be learned or estimated, the reduced-rank LDA for $C > 2$ classes still corresponds to looking at the top d eigenvectors of Σ . That is to say, we transform the predictor variables via $x \mapsto U_d x$ followed by performing LDA on the transformed data. Similarly, the PCA transformation corresponds to using the top d eigenvectors of the pooled covariance matrix $\tilde{\Sigma} = \mathbb{E}[(X - \sum_c \pi_c \mu_c)(X - \sum_c \pi_c \mu_c)^\top]$ followed by performing LDA. Suppose we now compare LOL, rrLDA, and PCA in this multi-class setting. Let $A: X \mapsto AX$ be a linear transformation. Then by Eq. (11) and Eq. (12), the Chernoff information for the transformed data in this multi-class setting is

$$\min_{c \neq c'} \frac{1}{8} (\mu_c - \mu_{c'})^\top A^\top (A \Sigma A^\top)^{-1} A (\mu_c - \mu_{c'}).$$

We now see that, in the case of rrLDA and PCA the linear transformation A depends only on the covariance matrix Σ and $\tilde{\Sigma}$, respectively. That is to say, the linear transformation A does not depend on the choice of c and c' . In contrast, currently for LOL the linear transformation A depends on both Σ as well as $\mu_c - \mu_{c'}$. In other words, there is no single choice for A but rather that A changes as c, c' changes. Direct comparison, in the multi-classes setting, between LOL and either of rrLDA or PCA is thus an open problem that we leave for future work. Finally we note that if we allow the linear transformation for LOL to vary with the classes c and c' , i.e., taking a one-vs-one approach to multi-classes classification, then the results presented in this paper are valid for all pairs c, c' .

D.III Finite Sample Performance

We now consider the finite sample performance of LOL and PCA-based classifiers in the high-dimensional setting with small or moderate sample sizes, e.g., when p is comparable to n or when $n \ll p$. Once again we assume that $X|Y = i \sim \mathcal{N}(\mu_i, \Sigma)$ for $i = 0, 1$. Furthermore, we also assume that Σ belongs to the class $\Theta(p, r, k, \tau, \lambda)$ as defined below.

Definition Let $\lambda > 0$, $\tau \geq 1$ and $k \leq p$ be given. Denote by $\Theta(p, r, k, \tau, \lambda, \sigma^2)$ the collection of matrices Σ such that

$$\Sigma = V \Lambda V^\top + \sigma^2 I$$

where V is a $p \times r$ matrix with orthonormal columns and Λ is a $r \times r$ diagonal matrix whose diagonal entries $\lambda_1, \lambda_2, \dots, \lambda_r$ satisfy $\lambda \geq \lambda_1 \geq \lambda_2 \geq \dots \geq \lambda_r \geq \lambda/\tau$. In addition, assume also that $|\operatorname{supp}(V)| \leq k$ where $\operatorname{supp}(V)$ denote the non-zero rows of V , i.e., $\operatorname{supp}(V)$ is the subset of $\{1, 2, \dots, p\}$ such that $V_j \neq 0$ if and only if $j \in \operatorname{supp}(V)$.

We note that in general $r \leq k \ll p$ and $\lambda/\tau \gg \sigma^2$. We then have the following result.

Theorem 3 ([19]). *Suppose there exist constants M_0 and M_1 such that $M_1 \log p \geq \log n \geq M_0 \log \lambda$. Then there exists a constant $c_0 = c_0(M_0, M_1)$ depending on M_0 and M_1 such that for all n and p for*

which

$$\frac{\tau k}{n} \log \frac{ep}{k} \leq c_0,$$

there exists an estimate \hat{V} of V such that

$$\sup_{\Sigma \in \Theta(p, r, k, \tau, \lambda, \sigma^2)} \mathbb{E} \|\hat{V}\hat{V}^\top - VV^\top\|^2 \leq \frac{Ck(\sigma\lambda + \sigma^2)}{n\lambda^2} \log \frac{ep}{k} \quad (20)$$

where C is a universal constant not depending on p, r, k, τ, λ and σ^2 .

Theorem 3 then implies the following result for comparing the Chernoff information of the sample version of LOL against that for PCA.

Corollary 4. *Let $\Sigma \in \Theta(p, r, k, \tau, \lambda)$ as defined above. Suppose that $C(F_0^{(A)}, F_1^{(A)}) > C(F_0^{(B)}, F_1^{(B)})$ where A and B denote the LOL and PCA projection matrices based on the eigenvectors of Σ associated with the $d \leq r$ largest eigenvalues, i.e. $A = [\delta | V_{1:d-1}]$ and $B = V_{1:d}$. Then there exists constants M and c such that if $\log n \geq M \log \lambda$ and $\frac{\tau k}{n} \log \frac{ep}{k} \leq c$, then there exists an estimate \hat{V} of V such that, with $\hat{A} = [\hat{\delta} | \hat{V}_{1:d-1}]$ and $\hat{B} = [\hat{V}_{1:d}]$, we have*

$$\mathbb{E}[C(F_0^{(\hat{A})}, F_1^{(\hat{A})})] > \mathbb{E}[C(F_0^{(\hat{B})}, F_1^{(\hat{B})})]$$

The above corollary states that for $\Sigma \in \Theta(p, r, k, \tau, \lambda)$, then provided that the Chernoff information of the population version of LOL is larger than the Chernoff information of the population version of PCA, we can choose n sufficiently large (as compared to λ and τ and k) such that the expected Chernoff information for the sample version of LOL is also larger than the expected Chernoff information of the sample version of PCA. We emphasize that it is necessary that the LOL and the PCA version are both projected into the top $d \leq r$ dimension of the sample covariance matrices. The constants M and c in the statement of the above corollary are chosen so that M (which depends on M_0 and M_1 in the statement of Theorem 3) is sufficiently large and c (which depends on c_0) is sufficiently small to ensure that the bound in Eq. (20) is sufficiently small. If $C(F_0^{(A)}, F_1^{(A)}) > C(F_0^{(B)}, F_1^{(B)})$ and $\|\hat{V}\hat{V}^\top - VV^\top\|$ is sufficiently small, then $\mathbb{E}[C(F_0^{(\hat{A})}, F_1^{(\hat{A})})] > \mathbb{E}[C(F_0^{(\hat{B})}, F_1^{(\hat{B})})]$ as desired.

E Real-Data Performance Analysis

PCA, the industry-standard dimensionality reduction technique for high-dimensional problems, is compared to LOL, RP, and rLDA in terms of cross-validated classification error.

In the experiments, we used k fold cross-validation. Testing sets were rotated across all folds, with the training sets comprising the remaining $k - 1$ folds. A low-dimensional projection matrix \mathbf{A} is first learned through the training set, and the low-dimensional training points are then used to train an LDA classifier C . The testing points are embedded via \mathbf{A} , and classification error is determined using the trained classifier C .

Performance is assessed using Cohen's kappa [24], which normalizes the classification error typically between 0 (the classifier performs no better than the classifier which guesses the most-likely class from the training set, the `chance` classifier) and 1 (the trained classifier performs perfectly). Negative scores can be achieved if the trained classifier performs worse than the `chance` classifier. The effect size is measured as the difference between Cohen's kappa for the trained classifier after embedding

with $\text{PCA}_{\kappa}(\text{PCA})$ and the trained classifier after embedding with technique $\varepsilon, \kappa(\varepsilon)$. Table 1 provides details about each neuroimaging dataset.

| Problem | Sample Size (n) | Training Size* | # Features (p) | Classes (K) | Source |
|--------------|---------------------|----------------|---------------------|-----------------|----------------------|
| Templeton114 | 111 | 100 | $> 1.5 \times 10^8$ | 2 | MRN |
| BNU1 | 110 | 100 | $> 1.5 \times 10^8$ | 2 | CoRR [78] |
| BNU3 | 47 | 43 | $> 1.5 \times 10^8$ | 2 | CoRR [78] |
| SWU4 | 453 | 407 | $> 1.5 \times 10^8$ | 2 | CoRR [78] |
| KKI2009 | 42 | 38 | $> 1.5 \times 10^8$ | 2 | KKI [51] |
| Genomics | 340 | 306 | 745,184 | 2 | Douville et al. [31] |

Table 1: Table of datasets used in this study. The top 5 datasets (neuroimaging) are pre-processing by only registering the brains to the MNI152 template[47, 60, 65, 74]. The neuroimaging dataset comprises a total of 5 classification problems (5 datasets across a single sex classification task). The bottom dataset (genomics) is pre-processed by aligning sequencing data to 745,184 amplicons on the human genome. The genomics dataset comprises two benchmark classification problems (sex or age).

F Extensions to Other Supervised Learning Problems

F.I Large numbers of classes

Here, we explore an experiment in which the number of classes increases for a given simulation. We look at the multiclass hump- K problem, described in Section C. In this simulation, while the space spanned by the differences of means conveys more information than the directions of maximal variance, we expect that the shift in the means for a given class at a given dimension should also increase the variance fractionally in that direction as well. Figure 6A shows the simulation setup, for $K = 10$. Figure 6B indicates the misclassification rate as a function of Cohen’s Kappa. We use Cohen’s Kappa instead of the misclassification rate for direct evaluation since K varies widely across these simulations at a fixed number of total samples $n = 128$, making the difficulty of the problem as K increases two-fold: not only are there more classes, but there are also fewer examples of each class per simulation setting. In all cases, the best random classifier would be the classifier that continually guesses a single class continuously, which has expected accuracy of $\frac{1}{K}$. On all simulations, we see that both PLS and LOL rapidly approach a higher Kappa statistic (better performance relative the random classifier) as they learn the space spanned by the differences of means. PLS rapidly declines in performance as successive dimensions are added, and LOL sees a small performance decline, as successive dimensions should convey no information regarding the class. PCA is able to ultimately identify the space spanned by the differences of the means, but takes far more embedding dimensions to do so, and yields a lower Kappa statistic than either of the other two strategies.

F.II Hypothesis Testing

The utility of incorporating the mean difference vector into supervised machine learning extends beyond classification. In particular, hypothesis testing can be considered as a special case of classification, with a particular loss function. We therefore apply the same idea to a hypothesis testing scenario. The multivariate generalization of the t-test, called Hotelling’s Test, suffers from the same problem as does the classification problem; namely, it requires inverting an estimate of the covariance matrix,

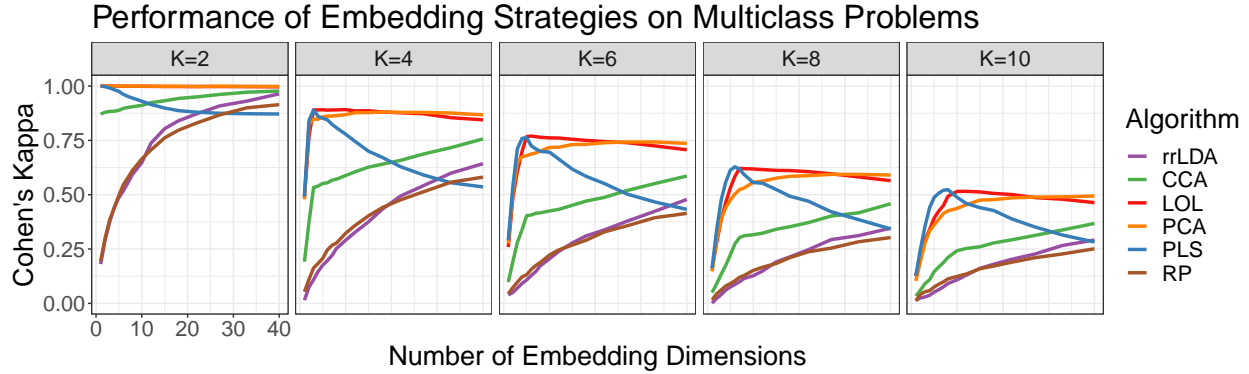


Figure 6: The Multiclass Hump Simulation. We show the results of the multiclass trunk problem, as the number of classes increases from 2 to 10, with the number of dimensions and the number of samples fixed. Effect size is measured with Cohen’s Kappa. `LOL` and `PLS` provide better performance over competing techniques including `PCA`, and this gap widens as the number of classes increases.

which would result in a matrix that is low-rank and therefore singular in the high-dimensional setting. To mitigate this issue in the hypothesis testing scenario, prior work applied similar tricks as they have done in the classification setting. One particularly nice and related example is that of Lopes et al. [56], who addresses this dilemma by using random projections to obtain a low-dimensional representation, following by applying Hotelling’s Test in the lower-dimensional subspace. Figure 7A and B show the power of their test (labeled `RP`) alongside the power of `PCA`, `LOL`, and `LFL` for two different conditions. In each case we use the different approaches to project to low dimensions, followed by using Hotelling’s test on the projected data. In the first example the true covariance matrix is diagonal, and in the second, the true covariance matrix is dense. The horizontal axis on both panels characterizes the decay rate of the eigenvalues, so larger numbers imply the data is closer to low-rank (see Methods for details). The results indicate that the `LOL` test has higher power for essentially all scenarios. Moreover, it is not merely replacing random projections with `PCA` (solid magenta line), nor simply incorporating the mean difference vector (dashed green line), but rather, it appears that `LOL` for testing uses both modifications to improve performance.

F.III Regression

High-dimensional regression is another supervised learning method that can use the `LOL` idea. Linear regression, like classification and Hotelling’s Test, requires inverting a matrix as well. By projecting the data onto a lower-dimensional subspace first, followed by linear regression on the low-dimensional data, we can mitigate the curse of high-dimensions. To choose the projection matrix, we partition the data into K partitions (we select $K = 10$ arbitrarily), based on the percentile of the target variable, we obtain a K -class classification problem. Then, we can apply `LOL` to learn the projection. Figure 7C shows an example of this approach, contrasted with `Lasso` and partial least squares, in a sparse simulation setting (see Methods for details). `LOL` is able to find a better low-dimensional projection than `Lasso`, and performs significantly better than partial least squares, for essentially all choices of number of dimensions to project into.

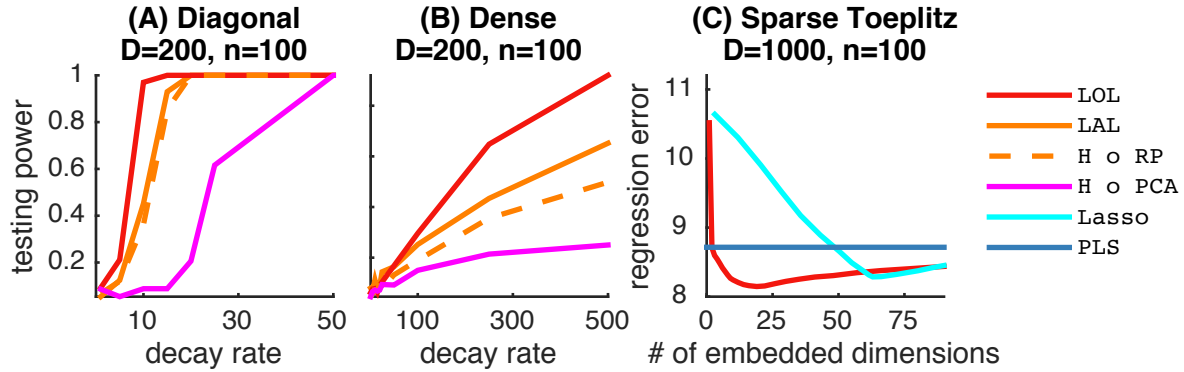


Figure 7: The intuition of including the mean difference vector is equally useful for other supervised manifold learning problems, including testing and regression. **(A)** and **(B)** show two different high-dimensional testing settings, as described in Methods. Power is plotted against the decay rate of the spectrum, which approximates the effective number of dimensions. `LOL` composed with Hotelling’s test outperforms the random projections variants described in [56], as well as several other variants. **(C)** A sparse high-dimensional regression setting, as described in Methods, designed for sparse methods to perform well. \log_{10} mean squared error is plotted against the number of projected dimensions. `LOL` composed with linear regression outperforms `Lasso` (cyan), the classic sparse regression method, as well as partial least squares (`PLS`; black). These three simulation settings therefore demonstrate the generality of this technique.

G The R implementation of `LOL`

Figure 8 shows the R implementation of `LOL` for binary classification using `FlashMatrix` [77]. The implementation takes a $D \times I$ matrix, where each column is a training instance and each instance has D features, and outputs a $D \times k$ projection matrix.

```
LOL <- function(m, labels, k) {
  counts <- fm.table(labels)
  num.labels <- length(counts$val)
  num.features <- dim(m)[1]
  nv <- k - (num.labels - 1)
  gr.sum <- fm.groupby(m, 1, fm.as.factor(labels, 2), fm.bo.add)
  gr.mean <- fm.mapply.row(gr.sum, counts$Freq, fm.bo.div, FALSE)
  diff <- fm.get.cols(gr.mean, 1) - fm.get.cols(gr.mean, 2)
  svd <- fm.svd(m, nv=0, nu=nv)
  fm.cbind(diff, svd$u)
}
```

Figure 8: The R implementation of `LOL`.

Pseudocode 1 Simple pseudocode for two class LOL on sample data.

Input: X a $p \times n$ matrix ($n \ll p$), where columns are observations; rows are features. An n length vector of observation labels, \mathbf{y} . An integer k to specify desired output dimension.

Output: $A \in \mathbb{R}^{p \times k}$

```
1: function LOL.TRAIN( $X, Y, k$ )
2:   for all  $j \in J$  do
3:      $n_j = \sum_{i=1}^n \mathbf{I}(y_i = j)$  ▷ sample size per class
4:      $\hat{\mu}_j = \frac{1}{n_j} \sum_{i=1}^n \mathbf{x}_i \mathbf{I}(y_i = j)$  ▷ class means
5:   end for
6:    $\hat{\delta} = \hat{\mu}_1 - \hat{\mu}_2$  ▷ difference of means
7:    $\hat{\delta} = \hat{\delta} / \|\hat{\delta}\|$  ▷ unit normalize difference of means
8:   for all  $i \in [n]$  do
9:      $\tilde{\mathbf{x}}_i = \mathbf{x}_i - \hat{\mu}_{y_i}$  ▷ class centered data
10:  end for
11:   $[\hat{\mathbf{u}}, \hat{\mathbf{d}}, \hat{\mathbf{v}}] = \text{svds}(\tilde{\mathbf{x}}, k - 1)$  ▷ compute top  $k$  singular vectors
12:   $A = [\hat{\delta}, \hat{\mathbf{u}}]$  ▷ concatenate difference of the means and the top  $k$  right singular vectors
13: end function
```
